

**LAWRENCE LIVERMORE NATIONAL LABORATORY YUCCA MOUNTAIN PROJECT
JUNE 1994 TECHNICAL HIGHLIGHTS AND STATUS REPORT
TABLE OF CONTENTS**

Executive Summary/Progress During Report Period	1
Deliverables	5
Variance Analysis/Explanations	6
WBS/Cost Performance Report	13
Cost/Full-Time Equivalent Report	15
Issues and Concerns	17
Technical Summary	18
1.2.1 Systems	18
1.2.2 Waste Package	22
1.2.3 Site Investigations	43
1.2.3.12 Waste Package Environment	45
1.2.5 Regulatory	55
1.2.9 Project Management	57
1.2.11 Quality Assurance	57
1.2.12 Information Management	58
1.2.13 Environment, Safety and Health	59
1.2.15 Support Services	59

LAWRENCE LIVERMORE NATIONAL LABORATORY (LLNL)
YUCCA MOUNTAIN SITE CHARACTERIZATION PROJECT (YMP)
STATUS REPORT

June 1994

EXECUTIVE SUMMARY

(Items Proposed for Reporting in YMSCO or OCRWM Reports)

1) **WBS 1.2.1.5, Special Studies:** A repository scale thermal-hydrological model was used to investigate the sensitivity of the relative humidity and temperature at various locations in the repository to the gas-phase diffusion efficiency. In general, for the factor of 10 range of diffusion investigated, the effect on temperature and relative humidity behavior is relatively minor. Re-wetting the reduced-relative humidity zone (also called the dry-out zone) back to humid conditions is affected by gas-phase re-wetting driven primarily by the binary diffusion of air and water vapor, and by liquid-phase re-wetting driven primarily by gravity drainage in fractures and matrix imbibition. Gas-phase re-wetting is likely to be the dominant re-wetting mechanism as the reduced-relative humidity zone re-wets to a value of about 70 to 80%. Subsequent re-wetting back to ambient relative humidity conditions (98.4%) is dominated by liquid-phase re-wetting.

2) **WBS 1.2.1.5, Special Studies:** Repository-scale thermal-hydrological calculations were conducted for six sets of matrix properties: those of the Reference Information Base and for the five sets of Topopah Spring welded tuff properties listed in Pruess and Tsang (1994) and based on Flint et al. (1993). The duration of the boiling period was found to be insensitive to the range of matrix properties considered. Five of the six property sets produced similar relative humidity conditions at the end of the boiling period for three Areal Mass Loadings (55.3, 110.5, and 150 metric tonnes uranium per acre). The sixth property set results in a substantially faster liquid-phase re-wetting rate and more humid conditions by the end of the boiling period, particularly for the low thermal load and for the outer 25% of the two higher thermal load repositories.

3) **WBS 1.2.2.3.1.1, Waste Form Testing - Spent Fuel:** Unsaturated dissolution tests at 90°C are in progress at Argonne National Laboratory to evaluate the long-term performance of spent fuel in the potential Yucca Mountain repository. These tests examine the leach/dissolution behavior of two types of well-characterized irradiated PWR fuels in three types of tests: saturated water vapor atmosphere, low drip rate of J-13 water equilibrated with tuff (0.075 mL/3.5 d), and a ten-fold higher drip rate. The ongoing tests have completed 21 months. As expected, the greatest mass of material is transported in the high-drip rate tests. The cesium transported was 1 µg for the high-drip rate tests, 0.3-0.7 ng for the low-drip rate tests, and 0.1-0.3 ng for the vapor tests; for comparison, the control test in the hot cell (with no spent fuel) measured less than a picogram of cesium.

4) **WBS 1.2.2.3.1.1, Waste Form Testing - Spent Fuel:** Parametric tests of unsaturated dissolution of UO₂ pellets exposed to dripping J-13 water at 90°C have been ongoing for 9 years at Argonne National Laboratory. These tests are designed to examine the dissolution behavior of UO₂, formation of alteration phases, release

rates, and mechanisms of uranium release, and serve as a pilot study for similar tests with spent nuclear fuel. Surface area normalized uranium release values have been measured for all Teflon-supported samples. Most tests are characterized by a period of rapid uranium release between one and two years of reaction. Uranium release rates during this interval were up to $14 \text{ mg}\cdot\text{m}^{-2}\cdot\text{d}^{-1}$, with most of this release being attributed to the spallation of UO_2 granules from the sample surface. Subsequent to the one-to-two year rapid release period, release rates for most tests decreased to an average of approximately 0.10 to $0.30 \text{ mg}\cdot\text{m}^{-2}\cdot\text{d}^{-1}$ throughout the duration of the tests.

5) WBS 1.2.2.3.1.2, Waste Form Testing - Glass: The N2 (Defense Waste Production Facility actinide-doped glass) unsaturated dissolution tests continue at Argonne National Laboratory. A scheduled solution sampling at 101 months was completed. In order to perform the sampling and retain the correct interchange of vessels, the stored liquid from the previous sampling period that was being saved for additional studies has been transferred to a glass storage vial. No problems were encountered, and the tests continue.

6) WBS 1.2.2.3.2, Metal Barriers: As a consequence of the Container Materials Workshop held in May, four bounding environments were identified that encompass the extremes that a metal barrier container could experience in the potential repository.

- A dilute groundwater, like that of Well J-13.
- A concentrated groundwater that would simulate a dry-out condition followed by resaturation with concentration of the ionic salts. Concentrations would be on the order of 20-100x those in the dilute groundwater.
- An acidified concentrated groundwater with pH as low as 2 that would simulate reactions between certain man-made materials and the water.
- An alkalized concentrated groundwater with pH as high as 12 that would simulate reactions between man-made materials, such as concrete, and the aqueous environment.

Long-term testing (on the order of five years or longer) in these four bounding environments will be useful in selecting materials for the container. The tests will be conducted at 60 and 90°C in the water, in the vapor phase above the water, and in some instances at the water line. Three groups of metals were also selected for testing:

- Corrosion allowance,
- Moderately corrosion resistant (e.g., 70/30 copper-nickel and Monel 400), and
- Highly corrosion resistant (e.g., Incoloy 825, Hastelloy C-22, Hastelloy C-4, Titanium Grade 12, and Titanium Grade 16).

7) WBS 1.2.2.3.2, Metal Barriers: In conjunction with the International Program, LLNL transported an array of metal barrier specimens for exposure in the New Zealand geothermal fields. Three sets of specimens were prepared from samples that were "on hand". These include flat coupons for weight loss, sandwich coupons for crevice observation, and stressed C-ring specimens for stress corrosion evaluation. Materials included two carbon steels, 316L stainless steel, Alloy 825, high purity copper, aluminum bronze, and 70-30 copper-nickel. On June 13, the first set of corrosion specimens was placed in Paraiki Hot Springs, where the environmental conditions are 89°C, pH 2, around 450 ppm chloride ion, and 1150

ppm sulfate ion. These are quite aggressive conditions which approximate one of the "bounding" environments planned for the long-term testing. The other sets of specimens will be placed in other locations in the New Zealand geothermal field so that a range of exposure conditions will be obtained

8) WBS 1.2.2.3.5, Non-Metallic Barrier Concepts: A preliminary study of the feasibility of fabrication of non-metallic barriers is nearly complete. General conclusions of this study are:

- Sufficiently large ceramic and ceramic coated vessels can be fabricated using currently available materials and techniques.
- Current industrial capacity is insufficient to handle the fabrication of large numbers of such vessels.
- Alumina based ceramics are probably the most suitable materials for non-metallic barriers.
- Experimental confirmation of the suitability of available materials is required.
- Final closure remains the weakest link in the use of non-metallic barriers due to average temperature limitations imposed by the zircaloy cladding.
- Thermal spray techniques are most promising both as fabrication and closure methods.

9) WBS 1.2.3.12.1, Chemical and Mineralogical Properties of the Waste Package Environment: Field-based experiments in New Zealand on dissolution and precipitation kinetics continue. Materials for sample holders have been emplaced in Paraiki Stream, in a pool at 89.1°C, pH 3.0, to evaluate the material durability. To date, all sample holder materials, except certain Fe- metals, have survived well. Mineral samples for kinetics measurements are ready for emplacement, once complete evaluation of sample holders is finished.

10) WBS 1.2.3.12.2, Hydrologic Properties of the Waste Package Environment: A series of thermo-hydrologic calculations were carried out for six sets of matrix properties of the TSw1 and TSw2 units; the properties were obtained from the Reference Information Base and from a recent Lawrence Berkeley Laboratory publication. These properties were shown to have a strong influence on both the time for return to a relative humidity that could accelerate corrosion and on the temperature at which the humidity returns. Since corrosion will be accelerated when both temperature and humidity are high, it is important to be able to accurately calculate these parameters.

11) WBS 1.2.3.12.3, Mechanical Attributes of the Waste Package Environment: Development of a Multipoint Borehole Laser EXtensometer (MBLEX) design continued in support of the Large Block Test, and several component parts for this system were ordered. This system was discussed with representatives of AECL, USBM, Bechtel Corp., and other interested parties to evaluate potential collaborations in its development.

12) WBS 1.2.3.12.4, Engineered Barrier System (EBS) Field Tests (Large Block Test): Engineering analysis of the capability of the load retaining frame, as designed, was completed. The load retaining frame design is not structurally adequate to contain the desired pressure of 600 psi. Modifications were proposed to retrofit the frame.

13) **WBS 1.2.5.3.4, Geologic and Engineering Materials Bibliography of Chemical Species (GEMBOCHS):** A revised set of element catalogs has been generated. The catalogs contain all thermodynamic data available in GEMBOCHS for compounds of the elements Tc, Th, U, Np, Pu, and Am. The catalogs are now available for remote electronic access via the anonymous GEMBOCHS ftp account.

14) **WBS 1.2.5.3.4, Geologic and Engineering Materials Bibliography of Chemical Species (GEMBOCHS):** The first edition of the new, stand-alone GEMBOCHS Data Catalog for the YMP-TDB was generated. This quarterly catalog, which covers the second quarter of 1994, includes an overview of the GEMBOCHS system, a discussion of recent accomplishments, and tables summarizing

- The types of thermodynamic data contained in GEMBOCHS,
- The specific chemical species and data contained in each of the seven thermodynamic data files currently provided for use with EQ3/6, and
- The literature sources for these data.

**LLNL Deliverables Met
(June 1994)**

None

**LLNL Deliverables Not Met
(June 1994)**

Milestone	WBS	Planned Date	Projected Date	Description	Comment
MOL45	1.2.2.3.2	01-31-94	07-29-94	Submit updated Metal Barriers SIP	Delayed by TPR & NWTRB preparation
MOL04	1.2.3.10.3.1	01-12-94	08-15-94	Document core flow experiment protocol	Delayed by equip.malfunction
MOL03	1.2.3.10.3.1	03-31-94	07-29-94	Report on colloid characterization	Delayed by equip.malfunction related to MOL04
MOL26	1.2.3.12.1	03-31-94	07-29-94	Topical Report on Near Field Geochemistry	Delayed by TPR & NWTRB preparation
MOL15	1.2.3.12.4	03-31-94	07-29-94	Large Block Excavated and Small Blocks Delivered to LLNL	Delayed by construction planning
MOL34	1.2.3.12.4	06-30-94	07-29-94	Pre-Test Calculations on Large Block Test	Will not impact LBT schedule
MOL73	1.2.3.12.5	05-31-94	07-29-94	Stability of Organic Compounds	Delayed by new ESF work
MOL91	1.2.5.4.2	03-31-94	07-29-94	Submit plan for code qualification	Individual Software Plan is currently in technical review
MOL89	1.2.5.4.2	06-30-94	08-31-94	YMIM Release, including User Manual	In final review

**LLNL Deliverables Scheduled for the Next Reporting Period
(July 1994)**

Milestone	WBS	Planned Date	Projecte d Date	Description	Comment
MOL94	1.2.2.3.2	07-29-94	07-29-94	Eng. Materials Characterization Report	
MOL24	1.2.3.12.1	07-29-94	07-29-94	Manuscript and Field Data of Preliminary Results of New Zealand Field Studies and Simulation	
MOL31	1.2.3.12.2	07-29-94	07-29-94	Impact of Heterogeneity on Heat Pipes and Buoyant Vapor Flow	

Yucca Mountain Site Characterization Project
 Variance Analysis Report
 Status Thru: 30-JUN-94

PARTICIPANT: LLNL PEM: SMITH

WBS: 1.2.2.3.1.1

WBS TITLE: WASTE FORM TESTING - SPENT FUEL

P&S ACCOUNT: 0L2311

FY 1994 Cumulative to Date								FY 1994 at Completion						
BCWS	BCWP	ACWP	SV	SV%	SPI	CV	CV%	CPI	BAC	EAC	VAC	VAC%	IEAC	TCPI
1334	1369	1199	45	2.6	102.6	170	12.4	114.2	1785	1780	5	0.3	1563	71.6

Analysis

Cumulative Cost Variance:

The cost variance is due to two FY93 summary accounts being carried over into FY94 awaiting completion of milestones. The milestones required reports from PNL that were delayed by 30 days and as a result were not received by LLNL until mid October. These reports were immediately processed by LLNL and submitted to the Project Office for review. No actual costs were incurred but earned value was calculated upon closing of these summary accounts. These FY93 accounts were not removed during the FY93 Close-Out exercise in PACs and will continue to contribute an inaccurate \$120k to both the cost and schedule variance. The correct cost variance is 50.

Cumulative Schedule Variance:

Same as above. The correct schedule variance is -85.

Variance At Complete:

Ray B. Stewart, July 15, '94

 P&S ACCOUNT MANAGER DATE

W. L. Blaine 7/15/94

 TPO DATE

Yucca Mountain Site Characterization Project
 Variance Analysis Report
 Status Thru: 30-JUN-94

PARTICIPANT: LLNL PEM: TYNAN WBS: 1.2.3.11.3

WBS TITLE: GEOPHYSICS-ESF SUPPORT SUBSURFACE GEOPHYSICAL TSTG

P&S ACCOUNT: 0L3B3

FY 1994 Cumulative to Date									FY 1994 at Completion					
BCWS	BCWP	ACWP	SV	SV%	SPI	CV	CV%	CPI	BAC	EAC	VAC	VAC%	IEAC	ICPI
128	128	77	0	0.0	100.0	51	39.8	338.1	180	129	51	28.3	108	100.0

Analysis

Cumulative Cost Variance:

Cumulative Schedule Variance:

Variance At Complete:

\$20k has been taken via CCB action. However, some of the funds will be used to offset a shortfall in WBS 1.2.3.5.2.2 which was only allocated \$25k. The proper accounts will be charged; 1.2.3.11.3 will underrun and 1.2.3.5.2.2 will overrun; the total costs will be \$205k, but with a different distribution than anticipated by YMSCO. These actions are by direction of the YMSCO Asst. Manager for Sci. Programs.

W. S. Lelanne 7/15/94
 P&S ACCOUNT MANAGER DATE

W. S. Lelanne 7/15/94
 TPO DATE

Yucca Mountain Site Characterization Project
 Variance Analysis Report
 Status Thru: 30-JUN-94

PARTICIPANT: LLNL PEM: SIMMONS WBS: 1.2.3.12.4

WBS TITLE: ENGINEERED BARRIER SYSTEM (EBS) FIELD TESTS

P&S ACCOUNT: 0L3C4

FY 1994 Cumulative to Date									FY 1994 at Completion					
BCWS	BCWP	ACWP	SV	SV%	SPI	CV	CV%	CP1	BAC	EAC	VAC	VAC%	IEAC	TCPI
1985	1798	1786	-187	-9.4	90.6	12	0.7	100.7	2530	3019	-489	-19.3	2512	59.4

Analysis

Cumulative Cost Variance:

Cumulative Schedule Variance:

Excavation delays and frame delivery postponement has delayed block characterization activity. Do not anticipate recovery within the current fiscal year.

Variance At Complete:

Variance at completion caused by current estimates for instrumentation and loading devices for procurement of the large block. The test is in a state of evolution as are the models being developed to interpret the data. Several additional channels are required in the data acquisition system. Side loading of the blocks initially was going to be accomplished by a single bladder. Complications in the fabrication of the bladder, arising from the need to insert instrumentation through the bladder, forced considerations of other options. The current resolution is to achieve loading by using several bladders. This increased cost was identified and discussed during the midyear review at YMSCO. Complications with frame fabrication are requiring addition of an LLNL project engineer and more design effort. Subcontractor underbid a fixed price contract and has stated that they are unable to complete frame within budget. LLNL is researching legal requirements and options to accomplish Large Block loading.

W. L. Selame 7/15/94
 P&S ACCOUNT MANAGER DATE

W. L. Selame 7/15/94
 TPO DATE

Yucca Mountain Site Characterization Project
 Variance Analysis Report
 Status Thru: 30-JUN-94

PARTICIPANT: LLNL PEM: SIMMONS WBS: 1.2.3.12.5
 WBS TITLE: CHAR. OF EFFECTS OF MAN-MADE MAT. ON CHEM/MIN. CHGS.
 P&S ACCOUNT: 0L3C5

FY 1994 Cumulative to Date									FY 1994 at Completion					
BCWS	BCWP	ACWP	SV	SV%	SPI	CV	CV%	CPI	BAC	EAC	VAC	VAC%	IEAC	TCPI
197	166	265	-31	-15.7	84.3	-99	-59.6	62.6	248	385	-137	-55.2	396	68.3

Analysis

Cumulative Cost Variance:

Cumulative Schedule Variance:

Variance At Complete:

Workscope was added for studies of diesel fuel impacts on the ESF. Additional funding of \$160k has been approved for transfer from headquarters but has not yet been applied at LLNL. LLNL cannot change BCWS until documentation is received.

W. L. Lohman 7/15/94
 P&S ACCOUNT MANAGER DATE

W. L. Lohman 7/15/94
 TPO DATE

Participant LLNL		Yucca Mtn. Site Char. Project-Planning & Control System										01-Jun-94 to 30-Jun-94		
Prepared - 07/14/94:11:43:58		PACS Participant Work Station (PPWS)										Page - 1		
		WBS Status Sheet (WBS02)										Inc. Dollars in Thousands		
WBS No.	- 1.2	WBS Manager												
WBS Title	- YUCCA MOUNTAIN PROJECT													
Parent WBS No.	-	Parent WBS Manager												
Parent WBS Title	-													
Statement of Work														
See the current WBS Dictionary														
Cost/Schedule Performance														
Id	Description	Current Period					FY1994 Cumulative to Date					FY1994 at Completion		
		BCWS	BCWP	ACWP	SV	CV	BCWS	BCWP	ACWP	SV	CV	BAC	EAC	VAC
1.2.1	SYSTEMS ENGINEERING	13	13	13	0	0	120	120	106	0	14	160	156	4
1.2.2	WASTE PACKAGE	302	270	290	-32	-20	2558	2630	2495	72	135	3445	3480	-35
1.2.3	SITE INVESTIGATIONS	520	479	575	-41	-96	4946	4681	4757	-265	-76	6348	7156	-808
1.2.5	REGULATORY	124	129	139	5	-10	1096	1051	1092	-45	-41	1462	1530	-68
1.2.9	PROJECT MANAGEMENT	102	102	121	0	-19	917	917	991	0	-74	1222	1292	-70
1.2.11	QUALITY ASSURANCE	53	53	47	0	6	486	486	394	0	92	650	634	16
1.2.12	INFORMATION MANAGEMENT	21	21	27	0	-6	187	187	181	0	6	250	252	-2
1.2.13	ENVIRONMENT, SAFETY, & HEA	2	2	4	0	-2	19	19	12	0	7	25	25	0
1.2.15	SUPPCRT SERVICES	32	32	45	0	-13	286	286	245	0	41	382	380	2
Total		1169	1101	1261	-68	-160	10615	10377	10273	-238	104	13944	14905	-961
Resource Distributions by Element of Cost														
Fiscal Year 1994														
Budgeted Cost of Work Scheduled														
	Oct	Nov	Dec	Jan	Feb	Mar	Apr	May	Jun	Jul	Aug	Sep	Total	
LBRHRS	8281	7278	7559	7901	7754	7742	7988	7922	7912	7794	7746	7454	93341	
LABOR	762	654	658	749	711	720	725	743	722	730	709	708	8591	
SUBS	109	298	264	233	315	269	218	206	226	200	142	169	2649	
TRAVEL	0	0	0	0	0	0	0	0	0	0	0	0	0	
OTHER	155	193	147	199	175	189	181	248	214	217	221	233	2	
CAPITAL	0	0	11	21	146	59	7	81	7	0	0	0	2	
Total BCWS	1026	1145	1080	1202	1347	1237	1131	1278	1169	1147	1072	1110	13944	

Participant LLNL		Yucca Mtn. Site Char. Project-Planning & Control System										01-Jun-94 to 30-Jun-94	
Prepared - 07/14/94:11:43:58		PACS Participant Work Station (PPWS)										Page - 2	
		WBS Status Sheet (WBS02)										Inc. Dollars in Thousands	
WBS No.		-YUCCA MOUNTAIN PROJECT											
Resource Distributions by Element of Cost													
Fiscal Year 1994													
Actual Cost of Work Performed													
	Oct	Nov	Dec	Jan	Feb	Mar	Apr	May	Jun	Jul	Aug	Sep	Total
LBRHRS	8301	6113	5630	6247	6390	7092	7097	7530	8036	0	0	0	62436
LABOR	762	413	383	497	513	552	513	558	594	0	0	0	4785
SUBS	114	303	254	233	315	246	218	101	135	0	0	0	1919
TRAVEL	0	0	0	0	0	0	0	0	0	0	0	0	0
OTHER	152	385	243	355	388	452	388	456	532	0	0	0	1
CAPITAL	0	0	11	21	138	33	15	0	0	0	0	0	218
Total ACWP	1028	1101	891	1106	1354	1283	1134	1115	1261	0	0	0	10273
Resource Distributions													
Fiscal Year 1994	Oct	Nov	Dec	Jan	Feb	Mar	Apr	May	Jun	Jul	Aug	Sep	Total
BCWS	1026	1145	1080	1202	1347	1237	1131	1278	1169	1147	1072	1110	13944
BCWP	1188	1062	944	1048	1810	1177	1036	1011	1101	0	0	0	10377
ACWP	1028	1101	891	1106	1354	1283	1134	1115	1261	0	0	0	10273
ETC	0	0	0	0	0	0	0	0	0	1516	1606	1510	4632
Fiscal Year Distribution													
	Prior	FY1994	FY1995	FY1996	FY1997	FY1998	FY1999	FY2000	FY2001	FY2002	FY2003	Future	At Complete
BCWS	11048	13944	43192	46455	35899	25532	17825	12021	8664	3594	823	705	219722
BCWP	10882	10377	0	0	0	0	0	0	0	0	0	0	
ACWP	10846	10273	0	0	0	0	0	0	0	0	0	0	
ETC	0	4632	42662	45613	34901	25892	18815	12262	9167	3624	823	7574	227084

YMP PLANNING AND CONTROL SYSTEM (PACS)

MONTHLY COST/FTE REPORT

PARTICIPANT: LLNL
 DATE PREPARED: 7/11/94

FISCAL MONTH/YEAR: JUNE, 1994

WBS ELEMENT	CURRENT MONTH END								FISCAL YEAR		
	ACTUAL COSTS	PARTICIPANT FTES	HOURS	SUBCONTRACT HOURS	PURCHASE COMMITMENTS	SUBCONTRACT COMMITMENTS	ACCRUED COSTS#	CAP EQPT ACCURAL	APPROVED BUDGET	CURRENT FY94 AFP	CUMULATIVE COSTS
1.2.1.5	12,600	0.70	104			0			160,000		104,000
SUBT 1.2.1	12,600	0.70	104	0	0	0	0	0	160,000	122,061	104,000
1.2.2.1	19,500	1.00	160		76	0	0		400,000		316,800
1.2.2.3.1.1	350,799	0.90	150	483	119	163,429	587,413		1,785,000		761,999
1.2.2.3.1.2	101,294	0.20	32		364	6,043	68,762		280,000		221,294
1.2.2.3.2	125,400	3.90	615		16,386	25,182	0		880,000		640,100
1.2.2.3.5	10,500	0.70	108		0	0	0		100,000		81,000
CAPITAL EQUIP.	0				9,366	0	0	0	91,000	132,823
SUBT 1.2.2	607,493	6.70	1,065	483	26,313	194,654	656,175	0	3,445,000	766,403*	2,155,016
1.2.3.12.1	184,800	2.40	377		4,786	77,263			610,000		577,800
1.2.3.12.2	66,800	2.90	467		2,327	0	0		861,000		590,900
1.2.3.12.3	28,900	1.40	213		4,335	0	1,600		230,000		153,500
1.2.3.12.4	187,400	9.30	1,668		7,106	353,102	35,979		2,530,000		1,335,000
1.2.3.12.5	37,400	1.60	257		85	0	28,732		248,000		214,800
1.2.3.10.3.1	26,800	1.50	239		6,696	0	4,607		392,000		201,100
1.2.3.10.3.2	28,100	0.70	175		2	0	0		301,000		140,500
1st SUBT 1.2.3	540,200	20.30	3,396	0	25,343	430,365	71,318	0	5,172,000		3,213,600
1.2.3.1	23,300	1.20	156		188	0	0		245,000		207,000
1.2.3.4.2	27,600	1.00	160		103	0	0		381,000		247,000
1.2.3.5.2.2	1,700	0.00	5		0	0	0		25,000		58,700
1.2.3.10.1	200	0.00	0		0	0	0		75,000		91,500
1.2.3.10.2	11,700	0.60	100		0	0	0		75,000		173,400
1.2.3.11.3	1,400	0.10	10		36,525	0	0		80,000		24,000
CAPITAL EQUIP.	0	0.00	0		16,650	0	0		15,000	0
2nd SUBT 1.2.3	65,900	2.90	431	0	53,466	0	0	0	1,081,000	1,116,109	802,300
1.2.5.1	7,300	0.30	52		0	0	0		150,000		95,500
1.2.5.2.2	22,600	1.10	182		0	0	0		240,000		262,900
1.2.5.3.4	23,300	1.50	236		4,687	0	0		342,000		203,600
1.2.5.3.5	6,300	0.40	72		0	0	0		50,000		35,900
1.2.5.4.2	104,400	5.20	823		1,490	0	0		660,000		509,100
1.2.5.5.2	-100	0.00	0		0	0	0		20,000		6,800
CAPITAL EQUIP.	0				0	0	0	0	..	34,000	0
SUBT 1.2.5	163,800	8.50	1,365	0	6,177	0	0	0	1,462,000	1,294,237	1,113,600

YMP PLANNING AND CONTROL SYSTEM (PACS)

MONTHLY COST/FTE REPORT

PARTICIPANT: LLNL
 DATE PREPARED: 7/11/94

FISCAL MONTH/YEAR: JUNE, 1994

WBS ELEMENT	CURRENT MONTH END							FISCAL YEAR			
	ACTUAL COSTS	PARTICIPANT FTES	HOURS	SUBCONTRACT HOURS	PURCHASE COMMITMENTS	SUBCONTRACT COMMITMENTS	ACCRUED COSTS#	CAP EQPT ACCURAL	APPROVED BUDGET	CURRENT FY94 AFP	CUMULATIVE COSTS
1.2.9.1.2	58,800	1.90	293		11	0	0		621,000		465,700
1.2.9.2.2	61,500	4.90	787		1,366	0	49		601,000		523,200
SUBT 1.2.9	120,300	6.80	1,083	0	1,377	0	49	0	1,222,000	1,057,912	988,900
1.2.11.1	46,200	1.70	281		11,200	0	0		650,000		392,500
SUBT 1.2.11	46,200	1.70	281	0	11,200	0	0	0	650,000	609,812	392,500
										(FUNDED UNDER 1.2.16)	
1.2.12.2.2	15,500	0.80	127		0	0	0		116,000		81,800
1.2.12.2.3	10,400	0.30	48		0	0	0		134,000		96,400
SUBT 1.2.12	25,900	1.10	175	0	0	0	0		250,000	215,606	160,200
										(FUNDED UNDER 1.2.17)	
1.2.13.2.5	2,500	0.10	20		0	0	0		25,000		10,900
SUBT 1.2.13	2,500	0.10	20	0	0	0	0	0	25,000	18,750	10,900
1.2.15.2	38,200	3.00	749		99	0	0		290,000		184,800
1.2.15.3	7,900	0.10	24		0	0	0		92,000		59,100
SUBT 1.2.15	46,100	3.10	773	0	99	0	0	0	382,000	300,010	243,900
TOTAL LLNL	1,630,993	52	8,691	483	123,975	625,019	727,542	0	13,849,000	4,734,397	9,205,916

* This work was moved to WBS 1.2.3; however, funding for this work remains in Budget and Report Category DB010202 in the AFP.

**** Capital equipment budgets are included in the individual WBS Elements.

Per instructions letter dated 4/27/93 V.F. Iorii to W. L. Clarke

Issues and Concerns

Work conducted by the Spent Fuel Oxidation and Spent Fuel Dissolution tasks has been affected by a suspension of radiological work in Bldg. 325 at Pacific Northwest Laboratories (PNL). Work conducted by the YMP was not a contributory element in the closure of the facility; however, this action has had a significant impact on our work schedule. The program manager has requested formal documentation of the justification for the building closure. This justification will be provided to LLNL and placed in the project records. PNL Line Management has taken an action item to provide this documentation. At this time, it is anticipated that the facility will reopen in August. PNL staff have placed a priority on restart of YMP work when the building reopens.

TECHNICAL SUMMARY

1.2.1. SYSTEMS ENGINEERING

1.2.1.1 Systems Engineering Coordination and Planning

No significant activities.

1.2.1.5 Special Studies

In order to augment the thermo-hydrological calculation support of the thermal loading systems study, we have also been conducting the calculations in the near-field/altered zone hydrology WBS (1.2.3.12.2) with the same set of thermal loading assumptions. We assume a Youngest Fuel First SNF receipt scenario with a 10-yr cut-off for the youngest fuel [referred to as YFF(10)] and account for the emplacement of BWR waste packages (WPs) containing 40 assemblies per WP, and PWR WPs containing 21 assemblies per WP. The waste receipt schedule was supplied by John King of M&O. Areal Mass Loadings (AMLs) of 24.2, 35.9, 55.3, 70, 83.4, 100, 110.5, and 150 MTU/acre have been analyzed assuming the matrix hydrological properties given in the Reference Information Base (RIB) and Klavetter and Peters (1986). This month we investigated the impact of (1) enhanced gas-phase diffusion (this WBS element), and (2) more recent matrix hydrological property data given in a recent draft report (Pruess and Tsang, 1994), and which are based on measurements by Flint and others (1983) (WBS 1.2.3.12.2).

The Impact of Enhanced Gas-Phase Diffusion

Tables 1 and 2 list the time required to attain the indicated values of relative humidity, RH , and the temperatures at which those values of RH are attained, for three values of the binary, gas-phase diffusion tortuosity factor, τ_{eff} , (0.2, 1, and 2), and for AMLs of 110.5 and 150 MTU/acre. In general, for this range of τ_{eff} , the dependence of temperature and relative humidity behavior on τ_{eff} is seen to be relatively minor.

Re-wetting the reduced- RH zone (also called the dry-out zone) back to humid conditions is affected by:

- gas-phase re-wetting driven primarily by the binary diffusion of air and water vapor, and
- liquid-phase re-wetting driven primarily by gravity drainage in fractures and matrix imbibition.

Modeling and laboratory studies conducted by LLNL have demonstrated that gas-phase re-wetting is likely to be the dominant re-wetting mechanism as the reduced- RH zone re-wets from low RH to an RH of about 70 to 80%. Subsequent re-wetting back to ambient RH conditions (98.4%) is dominated by liquid-phase re-wetting. Enhanced gas-phase diffusion has two general effects on dry-out and re-wetting behavior. First, it enhances the magnitude of dry-out during the boiling period, particularly at the outer edge of the repository. Second, it enhances the gas-phase re-wetting rate for RH up to about 70 to 80%. This second effect primarily pertains to the post-boiling period.

For the 110.5-MTU/acre case (Table 1), enhanced gas-phase diffusion tends to:

- modestly affect the time required to re-wet to $RH = 70$ and 80% for the inner 75% of the repository,
- modestly increase the time required to re-wet to $RH = 95\%$ for the inner 75% of the repository,
- modestly increase the time required to re-wet to $RH = 70, 80,$ and 90% for the outer 10% of the repository, and
- substantially increase the time required to re-wet to $RH = 95\%$ for the outer 50% of the repository

The relationship between temperature and RH is relatively insensitive to the magnitude of gas-phase diffusion over this range of τ_{eff} for the inner 75% of the repository. For a given value of RH , enhanced gas-phase diffusion results in lower temperatures for the outer 25% of the repository.

Table 1: AML = 110.5 MTU/acre								
Time required to attain the indicated relative humidity at various repository locations and the temperature at which that value of relative humidity is attained for 22.5-yr-old SNF, $k_b = 280$ millidarcy, and three gas-phase diffusion tortuosity factors, τ_{eff} .								
The locations are identified as the fraction of the repository area enclosed, with 0 percent corresponding to the repository center, and 100 percent corresponding to the outer perimeter.								
Table 1a: $\tau_{eff} = 0.2$								
Fraction of repository area enclosed (%)	Time required to attain the indicated relative humidity (yr)				Temperature at which the indicated relative humidity is attained ($^{\circ}C$)			
	70%	80%	90%	95%	70%	80%	90%	95%
50	15,960	27,910	40,990	49,980	68	54	45	42
75	9540	15,520	24,950	32,590	76	64	53	48
90	3190	4890	7460	9890	93	82	73	68
97	1410	1810	2360	2890	106	101	93	88
Table 1b: $\tau_{eff} = 1.0$								
Fraction of repository area enclosed (%)	Time required to attain the indicated relative humidity (yr)				Temperature at which the indicated relative humidity is attained ($^{\circ}C$)			
	70%	80%	90%	95%	70%	80%	90%	95%
50	13,490	22,790	39,960	54,040	72	58	46	40
75	9160	15,570	27,210	37,890	76	63	51	45
90	3480	6170	11,400	16,740	90	77	64	57
97	1410	1970	3170	4760	106	98	85	76
Table 1c: $\tau_{eff} = 2.0$								
Fraction of repository area enclosed (%)	Time required to attain the indicated relative humidity (yr)				Temperature at which the indicated relative humidity is attained ($^{\circ}C$)			
	70%	80%	90%	95%	70%	80%	90%	95%
50	14,260	23,850	42,270	59,750	70	57	44	38
75	10,180	17,870	33,350	47,150	72	59	46	41
90	3920	7730	16,040	26,640	85	71	57	48
97	1490	2240	4490	8130	104	93	76	65

The temperature and RH behavior for the 150-MTU/acre repository (Table 2) shows similar sensitivity to the magnitude of gas-phase diffusion over this range of τ_{eff} . Enhanced gas-phase diffusion tends to:

- modestly affect the time required to re-wet to $RH = 70$ and 80% for the inner 75% of the repository,
- modestly increase the time required to re-wet to $RH = 70, 80,$ and 90% for the outer 10% of the repository, and

- substantially increase the time required to re-wet to $RH = 95\%$ for the outer 10% of the repository.

The relationship between temperature and RH is relatively insensitive to the magnitude of gas-phase diffusion over this range of τ_{eff} for the inner 75% of the repository. For a given value of RH , enhanced gas-phase diffusion results in lower temperatures for the outer 10% of the repository.

Table 2: AML = 150 MTU/acre								
Time required to attain the indicated relative humidity at various repository locations and the temperature at which that value of relative humidity is attained for 22.5-yr-old SNF, $k_b = 280$ millidarcy, and three gas-phase diffusion tortuosity factors, τ_{eff} .								
The locations are identified as the fraction of the repository area enclosed, with 0 percent corresponding to the repository center, and 100 percent corresponding to the outer perimeter.								
Table 2a: $\tau_{eff} = 0.2$								
Fraction of repository area enclosed (%)	Time required to attain the indicated relative humidity (yr)				Temperature at which the indicated relative humidity is attained ($^{\circ}C$)			
	70%	80%	90%	95%	70%	80%	90%	95%
50	20,630	34,850	50,920	64,120	68	52	45	41
75	16,400	24,520	32,700	43,360	70	59	51	46
90	8660	12,090	16,520	19,780	81	72	64	59
97	4330	6020	8180	10,060	93	84	77	72
Table 2b: $\tau_{eff} = 1.0$								
Fraction of repository area enclosed (%)	Time required to attain the indicated relative humidity (yr)				Temperature at which the indicated relative humidity is attained ($^{\circ}C$)			
	70%	80%	90%	95%	70%	80%	90%	95%
50	18,860	29,280	47,690	61,630	70	57	45	41
75	14,670	22,760	34,660	42,180	73	60	50	45
90	8790	13,210	19,810	27,190	79	69	59	52
97	4650	7050	10,970	14,340	88	78	69	63
Table 2c: $\tau_{eff} = 2.0$								
Fraction of repository area enclosed (%)	Time required to attain the indicated relative humidity (yr)				Temperature at which the indicated relative humidity is attained ($^{\circ}C$)			
	70%	80%	90%	95%	70%	80%	90%	95%
50	19,470	29,380	48,260	64,180	69	56	45	41
75	15,390	23,380	36,100	45,900	71	59	48	44
90	9610	14,520	23,170	29,140	76	66	55	50
97	5310	8420	13,500	18,330	84	74	64	57

Sensitivity of Relative Humidity Conditions at the End of the Boiling Period to Matrix Properties

This month's near-field/altered zone hydrology report discusses the sensitivity of temperature and relative humidity behavior to the matrix hydrological properties assumed for the TSw1 and TSw2. Repository-scale calculations were repeated for the five sets of matrix properties for the Topopah Spring welded tuff (Table 7 in Section 1.2.3.12.2) that are listed in Pruess and Tsang (1994) and based on Flint et al. (1993). Rather than repeat the details of that section, we focus here on the relative humidity conditions at the end of the boiling period.

Table 3 summarizes the duration of the boiling period at various repository locations and the RH attained at the end of the boiling period for the "reference" case based on the matrix hydrological properties obtained from the RIB and Klavetter and Peters (1986)] for AMLs of 55.3, 110.5, and 150 MTU/acre. The bulk permeability, k_b , is

280 millidarcy for all of these calculations. Table 4 summarizes the same information for the five sets of more recent matrix property data listed in Pruess and Tsang (1994) and based on Flint et al. (1993).

Table 3			
Duration of the boiling period at various repository locations and the relative humidity attained at the end of the boiling period for 22.5-yr-old SNF, various Areal Mass Loadings, $k_b = 280$ millidarcy, and assuming the matrix properties from Klavetter and Peters (1986) for the TSw1 and TSw2 units. The locations are identified as the fraction of the repository area enclosed, with 0 percent corresponding to the repository center, and 100 percent corresponding to the outer perimeter			
Fraction of repository area enclosed (%)	Duration of the boiling period (yr) and the relative humidity (%) at the end of the boiling period for indicated AMLs		
	55.3 MTU/acre	110.5 MTU/acre	150 MTU/acre
50	1760 yr 81%	6130 yr 44%	9590 yr 47%
75	1160 yr 84%	4290 yr 51%	7210 yr 45%
90	440 yr 93%	2870 yr 68%	5010 yr 54%
97	80 yr 98.5%	2150 yr 87%	3960 yr 67%

Table 4					
Duration of the boiling period at various repository locations and relative humidity attained at the end of the boiling period for 22.5-yr-old SNF, $k_b = 280$ millidarcy, and matrix properties for the TSw1 and TSw2 units obtained from the indicated sources. The locations are identified as the fraction of the repository area enclosed, with 0 percent corresponding to the repository center, and 100 percent corresponding to the outer perimeter					
Table 4a: AML = 55.3 MTU/acre					
Fraction of repository area enclosed (%)	Duration of the boiling period (yr) and the relative humidity (%) at the end of the boiling period for the indicated sources of TSw1 and TSw2 matrix properties				
	LBL-USGS-3.2	LBL-USGS-3.5	LBL-USGS-3.1/3.6	LBL-USGS-3.4	LBL-USGS-3.3
50	1660 yr 97.5%	1730 yr 82%	1770 yr 78%	1760 yr 77%	1780 yr 76%
75	1100 yr 98.2%	1140 yr 85%	1190 yr 79%	1180 yr 79%	1180 yr 76%
90	430 yr 98.8%	420 yr 95.8%	430 yr 89%	440 yr 86%	440 yr 83%
97	90 yr 98.9%	80 yr 98.8%	80 yr 98.7%	90 yr 97.6%	90 yr 95.7%
Table 4b: AML = 110.5 MTU/acre					
Fraction of repository area enclosed (%)	Duration of the boiling period (yr) and the relative humidity (%) at the end of the boiling period for the indicated sources of TSw1 and TSw2 matrix properties				
	LBL-USGS-3.2	LBL-USGS-3.5	LBL-USGS-3.1/3.6	LBL-USGS-3.4	LBL-USGS-3.3
50	5850 yr 68%	6110 yr 36%	6050 yr 38%	5930 yr 35%	6130 yr 36%
75	4020 yr 86%	4250 yr 48%	4200 yr 49%	4200 yr 46%	4280 yr 46%
90	2690 yr 95.3%	2800 yr 71%	2810 yr 67%	2850 yr 65%	2870 yr 63%
97	2070 yr 98.0%	2080 yr 93%	2110 yr 88%	2140 yr 85%	2170 yr 81%
Table 4c: AML = 150 MTU/acre					
Fraction of repository area enclosed (%)	Duration of the boiling period (yr) and the relative humidity (%) at the end of the boiling period for the indicated sources of TSw1 and TSw2 matrix properties				
	LBL-USGS-3.2	LBL-USGS-3.5	LBL-USGS-3.1/3.6	LBL-USGS-3.4	LBL-USGS-3.3
50	9320 yr 76%	9520 yr 36%	9370 yr 38%	9380 yr 37%	9360 yr 36%
75	6720 yr 89%	7030 yr 38%	6970 yr 39%	6980 yr 37%	7020 yr 36%
90	4420 yr 95.1%	4820 yr 55%	4860 yr 52%	4880 yr 50%	4920 yr 49%
97	3290 yr 96.5%	3720 yr 73%	3780 yr 66%	3810 yr 64%	3840 yr 62%

A comparison of Tables 3 and 4 indicates that the duration of the boiling period is insensitive to the range of matrix properties considered. A comparison of Tables 3 and 4 also indicates that with the exception of LBL-USGS-3.2, the remaining 4 LBL-USGS cases and the reference case result in very similar *RH* conditions at the end of the boiling period. Both of these observations apply to all three AMLs. Because

LBL-USGS-3.2 results in a substantially faster liquid-phase re-wetting rate, it results in relatively humid conditions by the end of the boiling period. This observation is particularly applicable to the entire 55.3-MTU/acre repository and to the outer 25% of the 110.5- and 150-MTU/acre repositories. Relative to the reference matrix hydrological property case, the following observations apply to the end of the boiling period for the 55.3-MTU/acre repository:

- LBL-USGS-3.2 results in more humid conditions,
- LBL-USGS-3.5 results in nearly the same *RH* conditions, and
- LBL-USGS-3.1/3.6, LBL-USGS-3.4, and LBL-USGS-3.3 result in slightly less humid conditions.

Relative to the reference matrix hydrological property case, the following observations apply to the end of the boiling period for the inner 75% of the repository for 110.5 and 150 MTU/acre repositories:

- LBL-USGS-3.2 results in more humid conditions and
- LBL-USGS-3.5, LBL-USGS-3.1/3.6, LBL-USGS-3.4, and LBL-USGS-3.3 result in less humid conditions.

In general, we observe that relative humidity behavior during the above-boiling period is much less sensitive to the matrix property data than during the post-boiling period.

It should be emphasized that Tables 1 through 4 are based on the smeared-heat-source, repository-scale model. Consequently, the listed value of *RH* is applicable to average liquid saturation conditions. Had a discrete representation of WPs been done, we would find that the local liquid saturation conditions surrounding the emplacement drift are generally drier than the average saturation conditions. In that regard, the repository-scale model indicates a *RH* that is wetter than the local value of *RH* in the emplacement drift. It should also be noted that thermo-hydrological heterogeneity and variability in the heat output among the WPs will cause local behavior to deviate from average behavior.

1.2.1.6 Configuration Management

No significant activity.

1.2.2. WASTE PACKAGE

1.2.2.1 Waste Package Coordination and Planning

Several LLNL staff members attended the fifth Design Integration Workshop held on June 29 in Pleasanton, CA. On the previous afternoon, a laboratory tour was conducted for some of the workshop participants and included stops to view the corrosion sensor laboratory, the slow crack growth test apparatus, and the thermogravimetric analysis unit. Several LLNL presentations were made during the tour and the workshop.

1.2.2.2 Waste Package Environment

This work is now being reported in WBS 1.2.3.12.

1.2.2.3 Waste Form and Materials Testing

1.2.2.3.1 Waste Form

1.2.2.3.1.1 Waste Form Testing - Spent Fuel

Work conducted by the Spent Fuel Oxidation and Spent Fuel Dissolution tasks has been affected by a suspension of radiological work in Bldg. 325 at Pacific Northwest Laboratories (PNL). Work conducted by the YMP was not a contributory element in the closure of the facility; however, this action has had a significant impact on our work schedule. The program manager has requested formal documentation of the justification for the building closure. This justification will be provided to LLNL and placed in the project records. PNL Line Management has taken an action item to provide this documentation. At this time, it is anticipated that the facility will reopen in August. PNL staff have placed a priority on restart of YMP work when the building reopens.

Spent Fuel Dissolution

No PNL activities are being reported this month due to a total shutdown of all radiological work in PNL Bldg. 325 for safety assessment. This will also further delay installation of the new liquid radioactive waste disposal holding tank for the analytical hot cells.

D-20-43, Unsaturated Dissolution Tests with Spent Fuel

Tests under unsaturated conditions at 90°C are in progress at Argonne National Laboratory (ANL) to evaluate the long-term performance of spent fuel in the potential Yucca Mountain repository. These tests examine the leach/dissolution behavior of two types of well-characterized irradiated PWR fuels, ATM-103 and ATM-106, in three types of tests: two with a saturated water vapor atmosphere, two with a drip rate of 0.075 mL/3.5 d, and two with a drip rate of 0.75 mL/3.5 d. A control test without fuel but with a 0.075 mL/3.5 d drip rate is also included. EJ-13 water for the tests came from well J-13 and was equilibrated with volcanic tuff for approximately 80 days at 90°C. The seven tests have undergone 21 months of testing at 90°C by the end of June.

The pH and carbon contents of the fluids for the tests (both the fluid supply and the leachate) are shown in Table 5. The pH for the drip tests, with the exception of the control test (CC1J1) which does not contain spent fuel, are 6.9 and 7.1. Since January 1994, a new batch of EJ-13 water has been used, and the pH of the EJ-13 introduced has ranged between 7.3 and 8.4. The two vapor tests (S6V1 and S3V1) have the lowest pH of the spent fuel tests, 6.1 and 6.7. Radiolysis appears to be the simplest explanation of the change in pH in the tests.

The organic carbon content (5 to 7 ppm) is relatively unchanged for the new EJ-13 water for the period January through April 1994. However, for the old EJ-13, the organic content has increased significantly, 128 ppm versus 5 to 7 ppm. For the high drip rate tests (S32J1 and S62J1), the organic and inorganic carbon content have decreased. For the two vapor tests, the organic carbon has increased, and

the inorganic carbon has decreased. The behavior of the carbon in the two low-drip tests (S31J1 and S61J1) appears similar to that in the vapor tests. Hypotheses have been proposed to explain the above results; these will be tested when analysis of the solid phases are conducted. The one result which is unexpected is the control tests which has a large increase in organic carbon and only a slight decrease in the inorganic carbon.

Test	pH	Organic Carbon, ppm	Inorganic Carbon, ppm	Total Carbon, ppm	Carbon Anion, ppm
EJ-13-old ^a	3.2	128	15.2	143	NA
EJ-13-1/94 ^b	8.4	5.1	20.2	25.7	NA
EJ-13-4/94 ^b	7.3	7.0	51.5	28.5	8.2
CC1J1-589 ^c	3.2	38.9	12.8	51.7	56.7
S3V1-580 ^c	6.1	11.1	3.7	14.8	12.5
S6V1-574 ^c	6.7	26.4	3.2	29.6	18.3
S31J1-568 ^c	7.1	11.8	3.8	15.8	9.4
S61J1-559 ^c	7.1	10.8	2.0	12.9	8.4
S32J1-581 ^d	6.9	3.4	3.2	6.6	6.5
S62J1-581 ^d	6.9	3.1	2.4	5.5	6.5

^a Results from aliquots from the previous EJ-13 bottle which was in the hot cell from 9/92 until 1/94.

^b Results from aliquots from the new EJ-13 bottle at successive dates of 1/94 and 4/94.

^c Results from leachate that was produced from both EJ-13 bottles.

^d Results from the removed 1/20/94 leachate. The new EJ-13 bottle was used after restart.

The anion composition of the spent fuel leachate as well as that of the EJ-13 water has been measured. The control test showed an increase in fluoride, chloride, nitrite, sulfate and formate from the EJ-13. Large increases in nitrite content are also seen in the two vapor tests, and the two low-drip tests. Smaller increases in nitrite are seen in the high-drip tests. The other differences may only denote variabilities inherent in the analyses. Measurements at three successive times did not reveal any trends. The up to a factor of two difference between the organic carbon content and the carbon anion content is attributed to the difference in detectability and accuracy of both techniques.

Gamma analysis of the leachates provides more definitive information. With only a few exceptions, the leachate quantities are one to seven orders of magnitude greater than that in the EJ-13 or in the control. As expected, the greatest mass of material is transported in the high-drip rate tests. The cesium transported was 1 µg for the high-drip rate tests, 0.3-0.7 ng for the low-drip rate tests, and 0.1-0.3 ng for the vapor tests. The americium, europium and cerium content in the base of the ATM-103 vapor test (S3V1) was one to two magnitudes greater than that found in the other vapor tests and in both of the low-drip rate tests. The reason for the difference from the low-drip rate test with ATM-103 (S31J1) is unknown. The results from the alpha and gamma analyses for the acid strip of the test vessels and the alpha results for the leachate should be available in the near future. At that time, the discrepancy may be resolved.

D-20-49.1, Unsaturated Dissolution Tests with Spent Fuel and UO₂

The objective of this Task is to evaluate the reaction of UO₂ pellets after exposure to dripping EJ-13 water at 90°C using the Unsaturated Test Method. More specifically, these tests are designed to examine the dissolution behavior of UO₂, formation of alteration phases, release rates, and mechanisms of uranium release, and serve as a pilot study for similar tests with spent nuclear fuel.

Surface area normalized uranium release values have been measured for all Teflon-supported samples up to the present 9-year (108 month) results. These data are being compiled for individual sampling periods and to track cumulative release trends. Most tests are characterized by a period of rapid uranium release between one and two years of reaction. Uranium release rates during this interval were up to 14 mg•m⁻²•d⁻¹, with most of this release being attributed to the spallation of UO₂ granules from the sample surface. A single sample (PMP8U-8) displayed a normalized release of 56 mg•m⁻²•d⁻¹, but this high value is believed to have arisen from the dissolution of secondary uranyl minerals during the final overnight acid strip of the test vessel components. Subsequent to the one-to-two year rapid release period, release rates for most tests decreased to an average of approximately 0.10 to 0.30 mg•m⁻²•d⁻¹ throughout the duration of the tests.

Spent Fuel Oxidation

Dry Bath Testing

A new fuel sample weighing balance, to replace the balance at PNL that has been used since testing began, was purchased and installed. The new balance has features which allow for faster weighings and automatic calibrations.

Purchase orders were placed to acquire parts for a new data acquisition system at PNL. The original acquisition system is much behind current technology and has several shortcomings. The new system will be installed during the interim shutdown which is scheduled for August.

Last year, a complete history of each test sample in the main part of the tests at PNL was entered into a computer spreadsheet. We are currently working on a similar history for the samples which make up the "special tests", i.e. drybaths 1, 8, and 9.

All drybaths at PNL are scheduled to be shut down on August 1 for an interim weighing of samples.

Thermogravimetric Apparatus (TGA)

The PNL Test Plan for Thermogravimetric Analyses of Spent Fuel Oxidation has been completed, reviewed internally, and sent to LLNL for approval. Revision of the PNL Technical Procedure is underway.

With the current hold on radiological work in PNL Bldg. 325, it has not been possible to complete the series of X-ray diffraction (XRD) analyses intended to determine if the observed loss of the $UO_{2.4}$ phase in spent fuel oxidized beyond an oxygen-to-metal ratio (O/M) of 2.4 is due to formation of an amorphous product or to a decrease in $UO_{2.4}$ crystallite size. The focus of this effort has shifted to transmission electron microscopy (TEM). An intensive effort is being made to produce suitable specimens of the highly friable oxidized fuel at $O/M > 2.4$ for TEM examination.

Materials Characterization Center (MCC) Hot Cell Activities

Planning for a fuel shipment to Argonne National Laboratory has been initiated. There is concern that this work may not be able to be accomplished during FY94 because of the time involved to obtain the needed shipping approvals and documentation. Preparations have begun at ANL to receive the spent fuel from the MCC. The MCC has asked for specifications; how much fuel, and in what form (rodlets or pellets). LLNL will respond with specifications in July.

1.2.2.3.1.2 Waste Form Testing - Glass

D-20-27, Unsaturated Testing of WVDP and DWPF Glass

The N2 (DWPF actinide-doped glass) tests continue. A scheduled solution sampling at 101 months was completed. Samples were taken for alpha spectroscopy, cation analysis using Inductively Coupled Plasma Mass Spectroscopy (ICP/MS), anions, carbon, and filtering to detect colloidal material. In order to perform the sampling and retain the correct interchange of vessels, the stored liquid from the 12/21/93 sampling period that was being saved for additional studies has been transferred to a glass storage vial. No problems were encountered, and the tests continue. Additional data from earlier test periods are being compiled.

The N3 (West Valley ATM-10 glass) tests continue as scheduled. A total of 79 months of testing have been completed. The cation release data for these tests have been compiled. Inclusion of the total contribution from the EJ-13 solution that was added during testing must be done to determine the final release values. This work plus the compilation of the actinide release data are now in progress.

Preparation for the next 6 month sampling period for these tests has been initiated, and the sampling is scheduled for July. The solution saved from the last sampling period, which contains colloidal material, will be saved in the event that the investigation of colloids is pursued.

D-20-70, Parametric Studies of WVDP and DWPF Glass

Sixteen tests continue with some in progress for up to 8 years. Two of these tests were sampled in June to prevent the water that has been collecting in the test vessels from contacting the glass. The sampling occurred without incident.

Tests on a variety of glasses exposed to 60 and 95% relative humidity at 70°C continue. No test terminations have been done for several years and none are planned for this year.

1.2.2.3.2 Metal Barriers

The purpose of the metallic barrier task is to characterize their behavior and determine corrosion rates and corrosion mechanisms, including the interaction between the metal containment barriers and the surrounding environment. Tests, modeling, and investigations are performed to determine this behavior. Conceptual models of corrosion processes are developed for use in evaluating waste package performance. This task provides considerable input on materials properties to the waste package and repository design teams, as well as to performance assessment.

Task Management and Quality Assurance (PACS OL232JCD)

A workshop was held May 10-12 in Pleasanton, CA to discuss plans for testing of container materials during the Advanced Conceptual Design (ACD) phase of the project. The workshop was attended by about 40 people, representing OCRWM, YMSCO, the M&O, LLNL, and various sub-contractors. An observer from the NWTRB attended also. The purpose of the workshop was to discuss what materials may be used for the multiple barrier concept that is the focused ACD approach, what environments are meaningful for testing, and what kinds of tests should be performed. Much of the emphasis was on "long term" testing (meaning up to 5 years of exposure) since recent project impetus is on substantially complete containment and on making an application for the construction authorization phase of licensing in 2001. Several informal talks were presented during the first two days of the workshop; then, on the morning of the third day, the participants were split into three groups:

- candidate materials,
- test environments, and
- test methods.

Each group made recommendations, which were reported back to the entire workshop body on the last afternoon. A summary of the workshop is being prepared, and the recommendations are being incorporated into the revised Metal Barrier Scientific Investigation Plan (SIP) and into the Engineering Materials Characterization Report.

In conjunction with the International Program, W. Bourcier transported an array of metal barrier specimens for exposure in the New Zealand geothermal fields. Three sets of specimens were prepared from samples that were "on hand". These include flat coupons for weight loss, sandwich coupons for crevice observation, and stressed C-ring specimens for stress corrosion evaluation. Materials included two-grades of carbon steel, 316L stainless steel, Alloy 825, high purity copper, aluminum bronze, and 70-30 copper-nickel. On June 13, the first set of corrosion specimens was placed in Paraiki Hot Springs, where the environmental conditions are 89°C, pH 2, around 450 ppm chloride ion, and 1150 ppm sulfate ion. These are quite aggressive conditions which approximate one of the "bounding" environments planned for the long-term testing. The other sets of specimens will be placed in other locations in the New Zealand geothermal field so that a range of

exposure conditions will be obtained. Because we did not have on hand specimens of some of the corrosion resistant metals, such as Hastelloy C-4, Hastelloy C-22, Titanium Grade 12 and Titanium Grade 16, we expect to obtain specimens of these materials for emplacement at a future date.

D. McCright and J. Farmer visited R. Russo at Lawrence Berkeley Lab on May 31 to discuss advanced techniques for sensitively measuring film growth on metals and alloys exposed to humid environments.

D. McCright attended the High Level Waste Conference May 23-26 in Las Vegas. He co-authored a paper with A. Roy and R. Fish (both of the M&O) on the container material selection process. R. Van Konynenburg presented a paper on the limitations of scientific prediction and participated in a panel discussion.

A QA grading package for Activity E-20-18F was completed, approved, and a copy forwarded to Argonne National Laboratory asking them to complete an ANL "preparedness review". The grading package covers the LLNL portion of the work, and the preparedness review is to show coordination of effort.

P. Fojas, a graduate student from the University of Nevada, Reno, began his summer assignment on May 25. He will work with G. Henshall, D. McCright, and others on development of experiments to provide parameters for the pitting corrosion model under development. D. Jones, a professor of metallurgical engineering at UNR, is working on a summer assignment to assist in preparation of the Engineering Materials Characterization Report.

A. Roy (M&O) visited with D. McCright and R. Van Konynenburg on June 13-14 to gather information on the physical and mechanical properties of the container candidate materials.

D. Stahl (M&O) visited with the Metal Barrier Principal Investigators on June 13-14 to discuss the workscope and budgets for the coming fiscal year. There were also a number of follow-up items from the May materials testing workshop that were discussed. These included the bounding environments, some specific corrosion tests, the proposed long-term comprehensive corrosion test, and milestones for FY95.

On a related project, D. McCright attended the Waste Acceptance Technical Review Group (TRG) meeting in Las Vegas on June 21-22. On June 22, the TRG took the public tour of Yucca Mountain to observe progress made on excavating the Exploratory Studies Facility and other related facilities. M. Voegle, SAIC, guided the TRG tour.

Prepare Planning Documents (PACS OL232LFF)

The purpose of this activity is to update the planning documents for the Metal Barriers Task, particularly the Scientific Investigation Plan (SIP) and any subordinate activity plans, to account for changes in the multi-purpose container, waste package, and repository designs. The current SIP was written for the Conceptual

Design phase, but the candidate materials and configuration of barriers proposed for ACD are significantly different, necessitating an extensive revision of the SIP.

Work continues on a re-write of the 1989 Metal Barrier SIP to include the materials and test plans specific to ACD. Recommendations resulting from the May Container Materials Workshop are being incorporated into the SIP, which is expected to be complete by late July. In addition to discussion of long-term corrosion tests, shorter term corrosion tests and other physical and mechanical evaluations are discussed, along with plans for modeling activities, degradation mode surveys, and inputs to selection criteria and material recommendations.

Because initiation of long-term tests is receiving a high priority in the planning process and will receive a great deal of attention if adequate funding is obtained to begin these tests in the early part of FY95, aspects of the planning for the long-term tests are discussed below. The revised SIP, as well as other planning documents, will reflect the level of attention that has been given to planning for the long-term comprehensive corrosion tests.

As a consequence of the May Container Materials Workshop, meetings of the staff continued with emphasis on test environments and test methods. In support of the long-term testing plan, J. Estill prepared a cost estimate of test specimen procurement and test vessel fabrication. Some 10,000 test specimens will be required for testing different corrosion specimen types in several test environments that bound the expected envelope of relevant Yucca Mountain repository conditions. Four bounding environments were identified that encompass the extremes that a metal barrier container could experience and reflect conditions that will cause high corrosion rates for some of the materials. About 24 test vessels will be required if two temperatures are used for four bounding environments, and each candidate alloy family is tested in a separate vessel. The numbers of test specimens and test vessels, and consequently the costs of the testing program, will be the subject of continuing dialogues between the principal investigators and LLNL project management. As a preliminary estimate, J. Estill prepared a cost analysis of specimen procurement from Metal Samples of Munford, Alabama, including estimates for glass vessels, thermocouples, heaters, and control/data acquisition equipment. The cost will range from \$100k to \$300k depending on specimen selection, e.g., U-bend vs. wedge open loaded (WOL) specimens for stress induced corrosion testing.

The four bounding environments are:

- A dilute groundwater, like that of Well J-13, which represents undisturbed aqueous conditions existing at Yucca Mountain.
- A concentrated groundwater that would simulate a dry-out condition followed by resaturation with concentration of the ionic salts. Concentrations would be on the order of 20-100x those in the dilute groundwater, and this would require continuing dialogue with PIs in the near-field environment on a detailed composition and the process for preparing this kind of environment. From a metallurgical performance point of view, it is important to retain the ratio of the various ionic species present in the dilute groundwater while recognizing the limitations on solubility of the various chemical species as the species are concentrated.

- An acidified concentrated groundwater that would simulate reactions between certain man-made materials and the water. The "man-made" materials are those that would be introduced into the repository during construction and operation and which would not be removed or inadvertently left behind when operations cease. Hydrocarbons, such as fuels, oils, hydraulic fluid, brake fluid, and many other compounds may react with water and steam at somewhat elevated temperatures to form organic acids. This environment would further simulate the acid producing metabolism products of certain kinds of microbiological organisms. Values of pH as low as 2 may occur under certain bounding conditions, and these would be aggressive to several of the metallic candidate materials.
- An alkalized concentrated groundwater that would simulate reactions between man-made materials, such as concrete, and the aqueous environment. Values of pH as high as 12 could occur. In general, these high pH values would be beneficial to preventing high rates of corrosion, even for carbon steel.

It is felt that long-term testing (on the order of five years or longer) in these four bounding environments will be useful in selecting materials for the container. It is planned to conduct the tests at 60 and 90°C in the water, in the vapor phase above the water, and in some instances at the water line.

During the May Container Materials Workshop, candidate materials for multiple barrier waste package containers were categorized into three groups:

- Corrosion allowance,
- Corrosion resistant, and
- An "intermediate" group of materials having properties in between those of the first two groups.

In later discussions between Metal Barriers Principal Investigators and M&O design staff, the suggestion was made to rename the "intermediate" group as "moderately corrosion resistant". This includes such materials as 70/30 copper-nickel and Monel 400. As a further distinction the corrosion resistant group, including materials such as Incoloy 825, Hastelloy C-22, Hastelloy C-4, Titanium Grade 12, and Titanium Grade 16 should henceforth be termed "highly corrosion resistant". Thus, the three groups are:

- Corrosion allowance,
- Moderately corrosion resistant, and
- Highly corrosion resistant.

E. Dalder clarified some nomenclature about candidate corrosion allowance materials that were discussed and recommended at the May Container Materials Workshop. The correct designations are: UNS G10200 cross-referenced to ASTM A516 Grade 55 for the wrought carbon steel, UNS J02501 cross-referenced to ASTM A27 Grade 70-40 for the centrifugal cast carbon steel, and UNS K21590 cross-referenced to ASTM A 387 Grade 22 for the nominal 2 1/4 Cr - 1 Mo alloy steel.

E. Dalder obtained technical performance information about the recently developed Grade 16 titanium, which is a Ti-base "lean" alloy, containing around 0.05% Pd. Ti Grade 16 was identified as a candidate material for a highly corrosion resistant metal barrier at the May Container Materials Workshop. The very small palladium addition increases the resistance to crevice corrosion, while maintaining a fully

alpha phase microstructure which promotes greater resistance to embrittlement due to hydride formation. Thus, the two potentially damaging corrosion related problems in using titanium are greatly reduced. As with other Ti-base materials, Grade 16 is exceptionally resistant to corrosion in saline environments and in acid environments. This material, like other grades of titanium, is also apparently immune to microbiologically influenced corrosion. The Canadian AECL program on spent fuel containers is considering Grade 16 Ti as a candidate material. The Grade 16 Ti material was developed by the titanium industry as a lower cost alternative to previous grades that contained significantly higher palladium levels.

Degradation Mode Surveys (PACS OL232LFA, Activity E-20-13)

The purpose of a degradation mode survey is to amass previously published information about a candidate material and its performance in a number of environments and applications, and to interpret this body of information in the context of a potential repository in Yucca Mountain. In many cases, the degradation mode survey indicates the ways in which a material can degrade and serves to indicate the rate and kind of degradation in environments that have some similarity to what a metal barrier may experience in the Yucca Mountain setting. Lack of information in many cases suggests what work will be required to determine the behavior of the candidate material in Yucca Mountain environments.

Currently, D. Bullen at Iowa State University is compiling a degradation mode survey on carbon steel and alloy steels, cast irons and alloy cast irons. Revision 1 of the draft degradation mode survey was received on May 20 and a copy was sent to YMSCO on May 31. The draft is undergoing review at LLNL and at YMSCO. E. Dalder is coordinating the reviews. Completion of this survey constituted completion of Milestone MOL46.

E. Dalder visited Iowa State University on June 9 and discussed with D. Bullen and associates the status of the current degradation mode survey on iron-base materials and what future surveys might be needed on other materials. One such material is Ni-base Alloy 400 (Monel 400). Previous degradation mode surveys have focused on copper-nickels (such as CDA 715: 70 Cu-30 Ni) and on the Ni-Cr-Fe-Mo alloys, including the commercial Hastelloys, Incolloys, and Inconels. A specific survey on Alloy 400 would close the information gap.

Performance Tests and Model Development (PACS OL232LFB, Activity E-20-16)

The purpose of model development is to develop a predictive tool that will enable use of experimental data and analyses to draw long-term assessment of the performance of candidate container materials under Yucca Mountain conditions. This work will ultimately describe the performance of the multiple barrier waste package container. As a first step in that direction, the modeling work has focused on pitting of a highly corrosion resistant barrier, such as one of the nickel-base or titanium-base candidate materials. While pitting corrosion is usually governed by electrochemical, chemical, and occasionally metallurgical parameters, an important aspect of pitting is "stochastic". Much of the modeling work is aimed at developing the stochastic aspect of pitting within the electrochemical and chemical parameters. G. Henshall is the Principal Investigator for the model development.

G. Henshall has prepared an article for the Materials Research Society Meeting on Nuclear Waste Disposal to be held in Kyoto, Japan in October of 1994. This article is entitled, "Stochastic Modeling of the Influence of Environment on Pitting Corrosion Damage of Radioactive Waste Containers", and has been submitted to YMSCO and LLNL for review and approval to publish.

Details of the Modeling: Exponential Birth Probability

G. Henshall has performed calculations over the past few months regarding the effects of wait time on pitting potential. These calculations have assumed that the birth probability, λ , depends upon the applied potential, E_{app} , according to the phenomenological expression:

$$\lambda \sim A (E_{app} - B) \quad (1)$$

where A and B are constants. As discussed elsewhere (Ref. 1), this is one of two expressions that have been used to model the electrochemical potential dependence of the birth probability. The other expression, which was the focus of more recent modeling effort, has the form

$$\lambda \sim C \exp(D E_{app}) \quad (2)$$

The values of A and B in equation (2) were selected based on two constraints: First, for the largest E_{app} used in the simulations, 0.02151 (arbitrary units), the value of λ must be the same as that for previous calculations using equation (1), i.e. $\lambda = 0.002151$. Second, the value of λ must decrease by a factor of 50 when E_{app} decreases by an order of magnitude from 0.02151. Using these computed values of C and D, simulations of the effect of wait time on pitting potential were performed as in previous months using 20 runs per simulation. No decay in λ with time was used (see the April 1994 report).

The pitting potential vs. wait time curves all had the same general shape, with variations only in the absolute values and the amount of scatter. Examples are shown in Figure 1 for the minimum wait time, t_{min} , and the median wait time, $\langle t_p \rangle$. Note how the pitting potential, $E_p (= E_{app})$, decreases as the wait time increases until the wait time reaches an asymptotic limit. At this point, wide variations in E_p result from the same wait time. Physically, these results do not appear to be plausible. They suggest that pitting would occur within a constant, finite wait time at arbitrarily low potentials.

The reason for the unusual behavior shown in Figure 1 is evident by plotting the birth probability as a function of E_{app} . The upper graph of Figure 2a shows that for E_{app} values below about 4×10^{-4} (arbitrary units), the birth probability reaches a limiting value. Therefore, in this regime, pits initiate after essentially the same wait time regardless of the applied potential. The reason for the behavior shown in this plot stems directly from equation (2). As shown in the semi-log plot on the lower half of Figure 2b, λ is clearly an exponential function of the applied potential (linear on the semi-log plot).

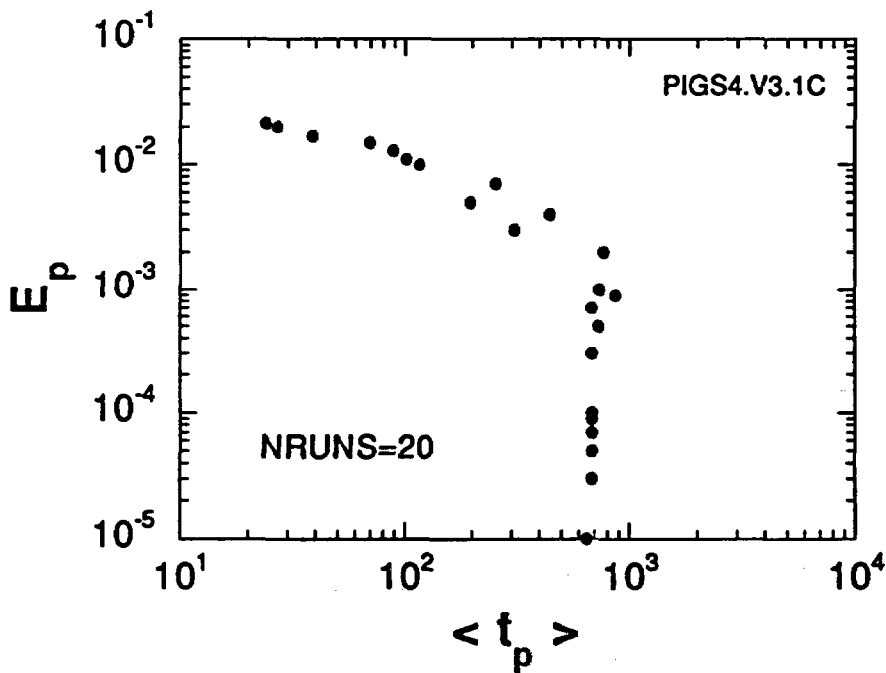
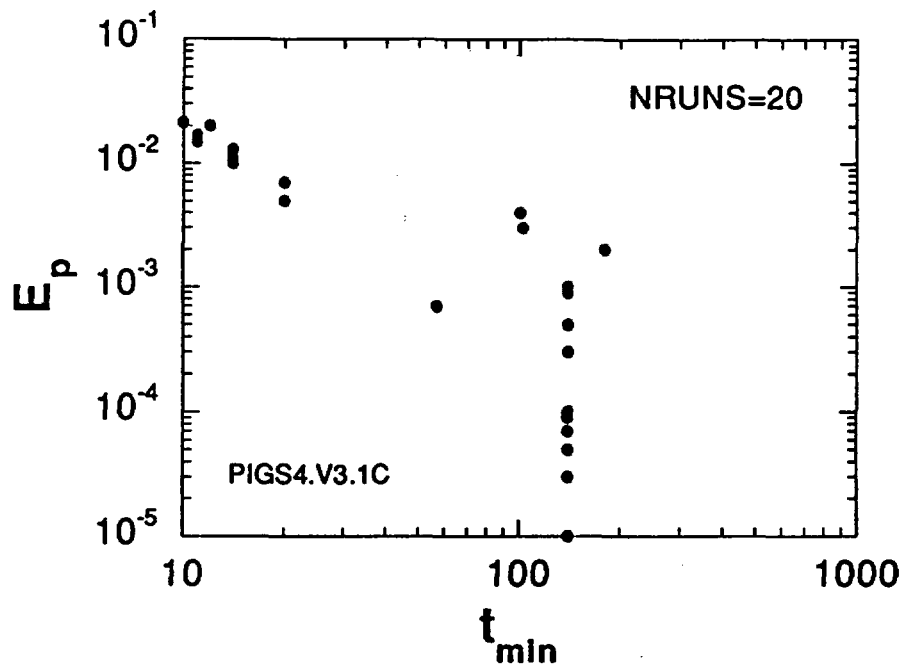


Figure 1. The variation in the pitting potential, E_p , as a function of t_{\min} and $\langle t_p \rangle$ for the case in which the birth probability is given by the exponential expression of equation (2). The units for potential and time are arbitrary.

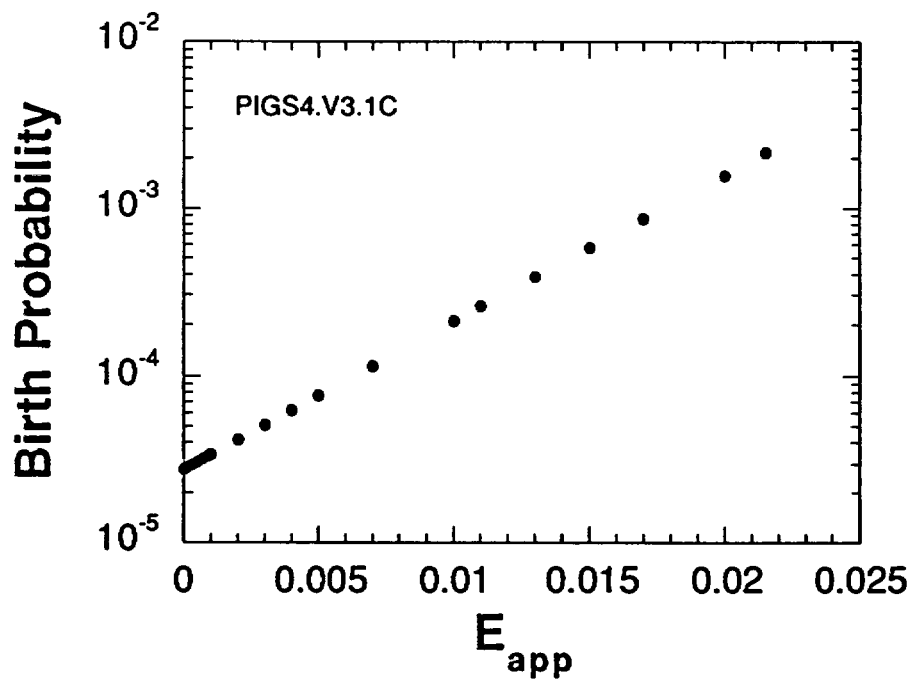
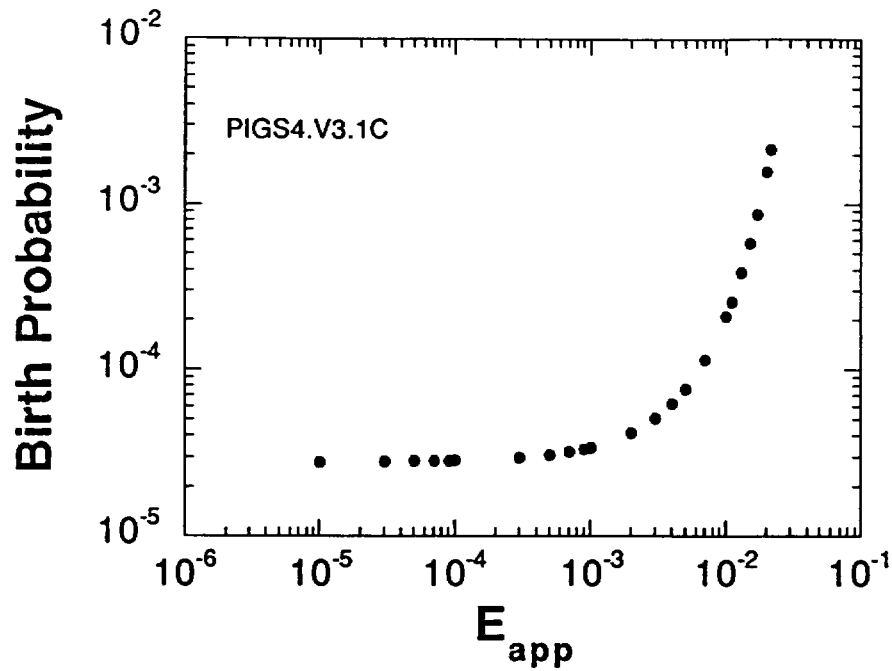


Figure 2. The variation in the birth probability as a function of the applied potential corresponding to the simulations depicted in Figure 1. The results are shown on log-log and semi-log coordinates axes. The units for potential are arbitrary.

Details of the Modeling: Potentiodynamic Pitting Experiment Simulation

Measurements of the pitting potential are often made using a potentiodynamic technique, rather than the potentiostatic one that has been simulated in previous months. Simulation of potentiodynamic experiments required the development of a new version of the Pitting Initiation and Growth Studies (PIGS) computer program and a program to construct histograms from an array of real numbers. Details of the new model and what its usefulness may be are given below.

In a typical potentiodynamic experiment, the applied potential, E_{app} , is swept from a low value, E_o , toward higher values at a constant velocity, v :

$$E_{app} = E_o + vt \quad (3)$$

where t is time. The potential at the time the first pit is detected is designated as the pitting potential, E_p . As discussed by Shibata and Takeyama (Refs. 2-4), the stochastic theory of pitting predicts that E_p is actually a distributed quantity for any given sweep velocity. From a simple algebraic stochastic theory based on birth processes only, Shibata and Takeyama (Refs. 2,4) deduced the most probable value of the pitting potential, \underline{E}_p , as a function of sweep velocity. The form of this relationship depends on the equation relating the birth probability, λ , and E_{app} . Both linear and exponential relationships between λ and E_{app} were observed (Refs. 2-4):

$$\lambda \sim \alpha (E_{app} - E_c) \quad (4a)$$

where α is a constant and E_c is the critical potential below which pit initiation cannot occur, or

$$\lambda \sim \gamma \exp (\beta E_{app}) \quad (4b)$$

where γ and β are constants. Using eqn. (4a) leads to (Refs. 2,4)

$$\underline{E}_p = (v/\alpha)^{1/2} + E_c \quad (5a)$$

while eqn. (4b) leads to

$$\underline{E}_p = [1/(\gamma \beta)] \ln(v/\gamma) \quad (5b)$$

Thus, a plot of \underline{E}_p vs. $v^{1/2}$ will yield a straight line if eqns. (4a) and (5a) are correct, or a plot of \underline{E}_p vs. $\log (v)$ will yield a straight line if eqns. (4b) and (5b) are correct.

Since the Monte Carlo model (PIGS) computes the generation of a stable pit using the concepts of embryo death and a critical embryo age in addition to embryo birth, the relationships between \underline{E}_p and the embryo birth probability, λ , are more complex than that assumed for deriving equations (5). Thus, it is necessary to determine if the $v^{1/2}$ and $\ln(v)$ relationships will be predicted by the more complex Monte Carlo model. If so, then the decision of which form of eqn. (4) to use within PIGS for a particular material-environment system can be made from plots of standard potentiodynamic experimental data.

To test this hypothesis, a series of simulations were performed in which the applied potential was swept according to eqn. (3). A particular sweep velocity was chosen, and a simulation was performed until the first stable pit was generated. The value of E_{app} at this time step, eqn. (3), was designated as E_p . This process was repeated with different random number "seeds" (Ref. 5) to produce one hundred separate E_p values for that particular sweep velocity. A histogram of these E_p values was generated, a smooth curve approximation was made, and the E_p value corresponding to the peak in this curve was designated as \underline{E}_p . Following Shibata (Ref. 2), the median pitting potential $\langle E_p \rangle$, was also calculated from the one hundred E_p values. This process was repeated for different values of sweep velocity, all other input parameters remaining constant, so that plots of \underline{E}_p and $\langle E_p \rangle$ vs. $v^{1/2}$ and $\log(v)$ could be constructed.

The results of such a numerical "experiment" are given in Fig. 3 for the case in which eqn. (4a) was used with $E_c = 0.0$. The initial potential, E_0 , in eqn. (1) was also set to 0.0. Both the median and the most probable pitting potentials clearly exhibit the $v^{1/2}$ dependence predicted by eqn. (5a) for the simple birth-only model. The \underline{E}_p results show somewhat more scatter than those for $\langle E_p \rangle$, perhaps due to the uncertainty in defining the smooth curve approximation to the histogram of E_p values. As predicted by eqn. (5a), the intercept at zero velocity is essentially zero. Also in agreement with the simple algebraic theory of Eqns. (5), plots (not shown here) of $\langle E_p \rangle$ and \underline{E}_p vs. $\log(v)$ were not linear.

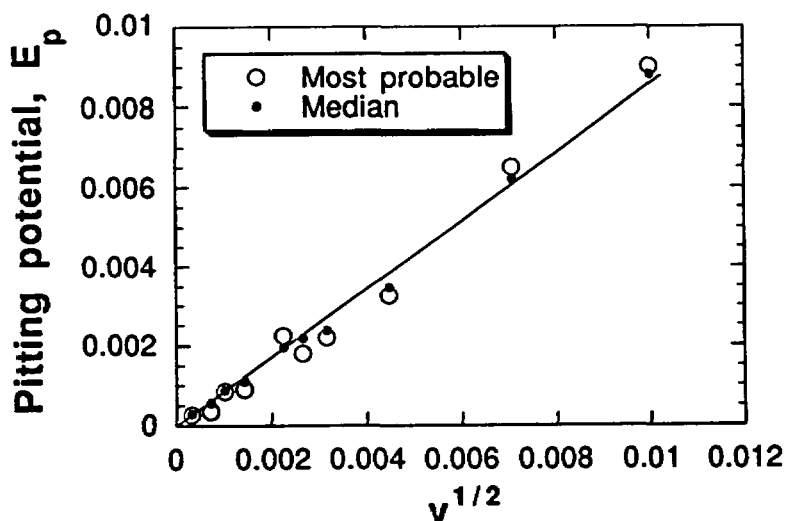


Figure 3. PIGS predictions of the most probable pitting potential, \underline{E}_p , and the median pitting potential, $\langle E_p \rangle$, as a function of the square root of the potentiodynamic sweep velocity for $E_c = 0$.

The results of a similar set of simulations are given in Fig. 4 for the case in which eqn. (4a) was used with $E_c = 0.002$. The initial potential; E_o in Eqn. (1), was set equal to 0.003. The median pitting potential clearly exhibits the $v^{1/2}$ dependence predicted by Eqn. (5a) for the simple birth-only model. The E_p results again show somewhat more scatter but also exhibit the linear dependence on $v^{1/2}$. Using linear regression analysis, a straight line was fit to the E_p data, and the intercept at zero sweep velocity was calculated to be 0.00208. The intercept predicted by Eqn. (5a) is $E_c = 0.002$; only 4% lower than that predicted by PIGS. Finally, neither the median nor the most probable values exhibit linear behavior on a plot (not shown here) of pitting potential vs. $\log(v)$.

Further simulations of this kind are planned in which Eqn. (4b) will be used. In this case, it is expected that Eqn. (5b) will better describe the results than Eqn. (5a). If so, then empirical potentiodynamic data could be used to determine whether Eqn. (4a) or (4b) should be used within the PIGS model (Ref. 1) to simulate pitting in any particular material-environment system.

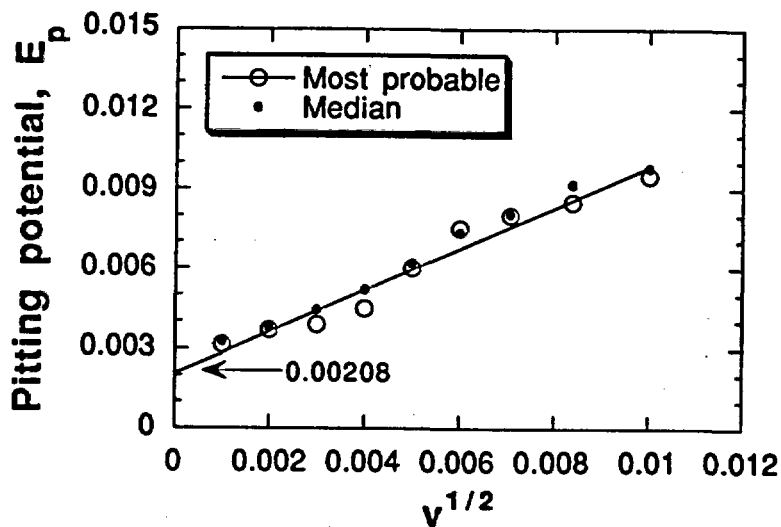


Figure 4. PIGS predictions of the most probable pitting potential, E_p , and the median pitting potential, $\langle E_p \rangle$, as a function of the square root of the potentiodynamic sweep velocity for $E_c = 0.002$.

Parameter Tests and Metal Degradation (PACS OL232LFC, Activity E-20-17)

There are currently two active parametric studies, one on thermogravimetric analysis and the other on corrosion sensor development, including support to the Large Block Test.

Thermogravimetric Analysis

The purpose of this work is to determine the limits where aqueous corrosion processes occur after emplacement of the waste package. The key parameters appear to be humidity, temperature, and surface conditions. The experimental work discussed in this section will indicate the inter-relationship between these parameters. Thermogravimetric analysis is a sensitive experimental method to discern the discontinuity in reaction rate corresponding to the transition from oxidation to corrosion.

In May, G. Gdowski and J. Estill performed several successful exploratory tests with the thermogravimetric analyzer. The previously mentioned problem of condensing water in the upper part of the apparatus was eliminated by modifying the heating of the exit port from the reactor and adjusting the flow rates of the reaction gas and the purge gas. In addition the width of the specimen was narrowed to eliminate possible interactions with sides of the reaction zone.

The exploratory tests were performed with commercially pure copper (CDA 102), the temperature range was 60 to 90°C, and the calculated relative humidities were 70 to 80%. The test times varied between 24 and 96 hrs. The tests consisted of holding the specimen at a constant temperature in a constant humidity environment. The flat plate specimen was suspended by a wire (platinum or high nickel alloy) attached to a hole that was drilled in one end of the plate. The specimen was thus oriented vertically.

It was found in every test that the most severe corrosion occurred at the bottom of the specimen. Depending on reaction conditions, the corrosion product varied between slight orange-brown discoloration to exfoliating black corrosion product. More severe corrosion occurred at longer test times and higher temperatures. Interestingly, under all test conditions, there were significant regions of the test specimen where visual inspection indicated very little oxidation.

It appears that the enhanced corrosion at the bottom of the specimen is due to water accumulation there. Unfortunately, real time visual monitoring of the specimen is not possible with the present test apparatus.

Exploratory testing of specimens with the thermogravimetric analyzer continued in June. These tests were performed with commercially pure copper (CDA 102; UNS# C10200), a carbon steel alloy (1020; UNS# G10200), and a Ni-Fe-Cr-Mo alloy (Incoloy 825, UNS# N08825).

A comparison of the three alloys tested under the same conditions (70°C, air with 60% relative humidity, 90-130 hrs.) showed that, as expected, the carbon steel was the most severely degraded, pure copper was less degraded, and Incoloy 825 showed no visible degradation. The carbon steel specimen was attacked over the whole specimen; however, there were regions of severe corrosion where the corroded material was exfoliated. The copper specimen had regions of very little attack and a smaller region of exfoliated black corrosion product. Optical inspection of the Incoloy 825 specimen indicated no corrosion. These tests also showed that

materials which were more aggressively attacked also absorbed the most water from the high humidity air.

A carbon steel specimen was also tested under lower humidity conditions (30% relative humidity) at 70°C for 90 hrs. Under these conditions, the weight gain was less than the detection limit of the instrument. Only a very small amount of oxidized material was optically visible. These tests showed the enhanced aggressiveness of the high humidity environment relative to the low humidity environment for carbon steel.

In July, a humidity sensor will be incorporated in the apparatus. Accurate humidity measurements in the reaction zone are necessary for an understanding of the interaction of water vapor with the test specimens. At present, the humidity in the reaction zone is obtained by calculation of test parameters.

Corrosion Sensor Development - Support to Large Block Test

The purpose of this activity is to develop sensors and methods to monitor atmospheric corrosion phenomena for prospective container materials, and also to investigate the rates and mechanisms of microbiologically-induced corrosion (MIC). Past work has centered on measurements in the liquid phase. Relatively little work has been done, relevant to the Yucca Mountain Site Characterization Project, on the application of electrochemical methods (and other sensors) in the gas phase, which is a more realistic corrosion environment for the repository. Our current efforts center around the development of microelectrode arrays for corrosion potential/rate measurements in the gas phase, initially to be used in the Large Block Test, and the use of the quartz crystal microbalance for studying MIC processes.

Metal Barrier personnel are developing sensors to support the Large Block Test (LBT). Principal Investigators M. Whitbeck and R. Glass are evaluating solid state iridium (IV) oxide pH sensors. Iridium wire coated with iridium (IV) oxide has been prepared by electrolysis and will be used in evaluating polymeric coatings for ion-exchange and protection.

Preliminary tests are underway to address the sensing of corrosion as either a rate or as corrosion potential. Initial tests used iron and stainless steel (304) wire (0.05 - 0.125 mm dia) free standing, mounted in epoxy or in epon. A silver wire serves as a reference electrode when coated with silver chloride. Both potentiodynamic and simple potential measurements are being evaluated. Typical preliminary results indicate that corrosion measurements are feasible when there is an adequate amount of. Problems encountered include fragility of the connections; future designs will include electrical connectors epoxied directly to the probe.

During June, the humidity chamber in LLNL Bldg. 241/high bay was made operational, and the corrosion microsensor work was begun in humid environments. Our initial emphasis is to develop integrated sensors which can detect changes in the "corrosivity" of an environment (e.g., pH changes; increases in the chloride ion concentration, etc.) and also monitor the environmental (corrosion) response of the container materials of interest. Ultimately, these sensors will be manufactured using state-of-the-art microfabrication methods developed in the electronics

industry. Currently, bundles of microwires are sealed in epoxy, with only the ends of the wires being exposed (disc sensors of micron dimensions). The initial work is being done with iron and AISI 316 stainless steel. We believe that we are getting reasonable responses (corrosion potentials) at high humidities for these materials. Humidities above 90% RH are being used because this is what is expected to be encountered in the geochemical holes of the Large Block Test and in unventilated drifts in Yucca Mountain. A computer, display, and data logger have been interfaced to the experimental apparatus for long-term measurement and real-time display of results. Sensors for atmospheric pH and chloride will be tested in July. The initial application for these sensors is the Large Block Test, which will be monitored for long-term geochemical changes which may influence corrosion (e.g., as a result of evaporation, percolation, and condensation). The LBT will also include monitoring the response of Monel 400, 70/30 alloy, and carbon steel.

The quartz crystal microbalance (QCM) arrived during June. This system consists of the AC-cut quartz crystals, the crystal interface, and the analyzer module. Electrodes are plated on both sides of the crystal (they come with platinum, but any other material can be plated on). When an ac voltage is applied the electrodes, a shear wave is set up in the quartz (piezoelectric effect). The frequency of crystal vibration is inversely proportional to the mass of the crystal. Corrosion processes can be monitored if the container material of interest is used for the electrodes. The material either gains or loses weight as it corrodes, causing a frequency change, and the corrosion rate can be directly determined. Sensitivities of ng/cm^2 are possible. Both atmospheric and liquid phase corrosion can be investigated. During June, this system was set up and interfaced to a computer. We have done a library search of microbes present at the Yucca Mountain site, and have begun efforts to obtain some of these microbes. We will use the QCM to evaluate the rates of microbiologically-induced corrosion in both the liquid and gas phase.

Crack Growth Tests (PACS OL232LFD, Activity E-20-18F)

The purpose of this work is to determine the stress corrosion susceptibility of candidate container materials under a variety of environmental, metallurgical, and mechanical stress conditions relevant to the repository. Stress corrosion is an important degradation mode that can affect both corrosion allowance and corrosion resistant materials. Work to date has focused on the corrosion resistant materials. A sensitive crack growth measurement apparatus, which operates under the principle of measuring minute changes in the electrical resistance of the test specimen as a crack propagates, is in use at Argonne National Laboratory (ANL) to measure crack growth on pre-cracked compact tension specimens.

ANL Principal Investigators D. Diercks and J. Park have renewed YMP-sponsored research activity on the determination of crack growth rates in candidate metal barrier waste container materials. Research activities under this renewed phase deal with fracture mechanics crack-growth-rate determinations on Types 304L and 316L stainless steels and Incoloy 825 under high stress ratios. In addition, tests will be conducted under low stress ratio conditions on Ti Grade 12, Hastelloy C-4, and the new heat of Incoloy 825. The Incoloy 825, Type 304L SS, and Type 316L SS are from different heats of material than those tested in the previous phase of this program, and the Titanium Grade 12, Hastelloy C-4, and Hastelloy C-22 are

new materials for the program. As stated in previous reports, all six of the alloys to be tested have been purchased. The alloys are in the form of plate, and it was confirmed that the chemical compositions of the alloys meet specifications.

Cross-sections of the Type 304L SS, Type 316L SS and Incoloy 825 plates were metallographically examined in May to determine grain or rolling direction because this information was not available through the vendor. The grains are equiaxed and no preferred rolling is apparent. The Type 304L SS material showed larger grains than the Type 316L SS, and sensitization is not observed in either material. Metallographic examinations of the Hastelloy C-4 and C-22 material were presented in earlier reports. The grain direction for Ti Grade 12 was provided by the vendor. Four 1T-compact tension specimens were machined from each of the six materials. The design of the specimens is in accordance with the ASTM E399 Standard, except for 1.27-mm deep side grooves at both sides and a small threaded hole on the front face for instrumentation.

Before SCC tests begin, the specimens are being fatigue cracked in air at room temperature to introduce a sharp starter crack for a length of 1.91 mm. In June, the specimens were fatigue pre-cracked for Titanium Grade 12, Hastelloy C-4, and Hastelloy C-22 materials. The fatigue-cracking was performed in air at room temperature under a cyclic load with a triangular load shape, load ratio of $R = 0.1-0.25$ and 1 Hz.

The Preparedness Review was performed this month, and the task at ANL is approved to initiate quality affecting (ANL QA level 1) activities.

Engineered Materials Characterization Report - EMCR (PACS OL232LFE)

The purpose of preparing the materials characterization report is to compile and synthesize information on the cogent properties of the candidate materials for the Waste Package and other Engineered Barrier System components. This report is planned to incorporate information on the important physical, mechanical, and chemical properties of the candidate materials, plus an outline of the long range and short range testing planned during ACD. Much of the long range testing plans were discussed in the Planning Documents Section above. The Engineered Materials Characterization Report (EMCR) will serve as input to the Basis For Design document for Waste Package design.

D. Jones (UNR) and R. Van Konynenburg are tasked to be co-authors of the Engineered Materials Characterization Report. The first draft of the report has a due date of the end of July.

References for WBS 1.2.2.3.2

1. G. Henshall, W. Halsey, W. Clarke, and R. McCright, University of California Lawrence Livermore Laboratory Report No. UCRL-ID-111624 (1993).
2. T. Shibata and T. Takeyama, *Corr.* **33**, p. 243 (1977).
3. T. Shibata, *Corr. Sci.* **31**, p. 413 (1990).
4. T. Shibata and T. Takeyama, in Proc. Second Japan-U.S.S.R. Corrosion Seminar, JSCE (1980) pp. 178.

1.2.2.3.3 Other Materials

This WBS element has not been funded in FY94.

1.2.2.3.4 Integrated Testing

This WBS element has been moved to WBS element 1.2.3.10.3; progress is reported in that element.

1.2.2.3.5 Non-Metallic Barrier Concepts

(PACS OL235JGD and OL235KKA)

The purpose of the non-metallic barriers task is to characterize the behavior of non-metallic materials, such as ceramics, and to determine degradation rates and mechanisms, including the interaction between the barrier and the surrounding environment. The work in the non-metallic barriers task parallels that in the metallic barriers task. One of the multiple barriers of the waste package container may be fabricated from a non-metallic material. A primary objective of this task is determination of the feasibility of making a non-metallic barrier as part of a waste package.

K. Wilfinger has begun to collate data gathered over the past 6 months in preparation for writing a final report on large scale non-metallic barriers and sealing with a projected completion date of August 1. He continues to seek published data and the confirmation of manufacturer claims. He attended the manufacturer's exposition at the ASM Thermal Spray Conference in Boston MA on June 21.

Current industry claims are that certain thermal spray techniques and materials can offer relatively thick, impervious coatings at up to 98% of theoretical density. High Velocity Oxy-Fuel (HVOF) sprayers produce the densest materials in most applications. Coatings are considered "thick" when they exceed 1 millimeter; however free standing structures up to 80 millimeters thick have been made successfully. Some coatings can be pre-stressed thermally to make them more resistant to inadvertent damage. Robotic systems can be constructed to apply coatings to the interior or exterior of large vessels. Sealing of an interior lining remains an issue, while an exterior coating on a metal vessel could be made to provide a "seamless" closure. A relative few manufacturers claim to be able to lay down coatings of alpha alumina rather than the gamma phase normally resulting from thermal spray techniques. Product samples have been requested for confirmation by x-ray diffraction.

Manufacturers of monolithic, castable, refractory liners fabricate parts up to 2.5x2.5x6.7 m (8'x8'x22') and several inches thick. This technology could be used to fabricate movable containers, but the materials used are hydrated calcium aluminate cements with about 15% of connected porosity. As such, they are unlikely to be of use in preventing transport of water and radionuclides. A substantial development effort would likely be required to overcome this.

General conclusions of this study are:

- Sufficiently large ceramic and ceramic coated vessels can be fabricated using currently available materials and techniques.
- Current industrial capacity is insufficient to handle the fabrication of large numbers of such vessels.
- Alumina based ceramics are probably the most suitable materials for non-metallic barriers.
- Experimental confirmation of the suitability of available materials is required.
- Final closure remains the weakest link in the use of non-metallic barriers due to average temperature limitations imposed by the zircalloy cladding.
- Thermal spray techniques are most promising both as fabrication and closure methods.

1.2.2.4 Design, Fabrication, and Prototype Testing

1.2.2.4.3 Container/Waste Package Interface Analysis

This WBS element has not been funded in FY94.

1.2.3 SITE INVESTIGATIONS

1.2.3.1 Site Investigations Coordination and Planning

No significant activity.

1.2.3.2 Geology

1.2.3.2.1.2.1 Natural Analogue of Hydrothermal Systems in Tuff

This WBS element has not been funded in FY94. Funding has been requested from the YMSCO WBS manager in order to write the Study Plan.

1.2.3.4 Geochemistry

1.2.3.4.2 Geochemical Modeling

The Independent Software Validation activity for EQ3/6 Version 7 is in the final stages. Work is now focused on writing the final report, which is close to completion.

Work is progressing on incorporating thermodynamic pressure corrections and a generic ion exchange model into EQ3/6 Version 8.0. The test case library is being enlarged to represent these new capabilities, as well as the new redox disequilibrium capability. A preliminary round of regression testing comparing version 8.0 with version 7.2a was conducted. A convergence problem exists in high concentration solutions and is still being diagnosed. Some new options have been added to EQ6 to make it more convenient for the user to remove minerals present in equilibrium with the aqueous solution. Also, the code will now automatically generate (if necessary) a chemical reaction for a user-defined reactant species, based on its specified chemical composition. Reactions are required

because of the way the code now tracks mass balances (in terms of chemical species as opposed to chemical elements). In addition, the major option switches in EQ3NR and EQ6 have been made common between the two codes, in order to make them easier to use. Previously, some switches had one meaning in EQ3NR and another in EQ6.

T. Wolery's work on QP 3.2 (the software quality procedure) was completed last month and the procedure has been issued. This task had caused a minor delay in progress on EQ3/6 Version 8.0.

1.2.3.5 Drilling

1.2.3.5.2.2 Engineering, Design, and Drilling Support

One logging session was conducted at USW SD9 on June 28. A downhole run performed a photographic inspection of the drill hole.

1.2.3.10 Altered Zone Characterization

1.2.3.10.1 Characterization Techniques for the Altered Zone

No significant activity.

1.2.3.10.2 Characterization of Thermal Effects on the Altered Zone Performance

Experiments to examine rock-water interaction in relevant lithologic units continue. The run products from the earlier completed experiment are being analyzed.

Bounding analyses for identifying the range of responses that may result from hydrothermal processes were conducted using the FEHM code. Specific attention has been paid to reaction product volumes, and assuming specific changes in porosity and permeability due to these interactions. The results of those simulations are being analyzed. They will be used to determine, for preliminary scenarios and reconnaissance studies, the degree to which changes in permeability during rock-water interaction might influence thermal evolution of the repository block.

The study plan for this WBS is being written and is expected to be ready for internal LLNL review in August 1994.

1.2.3.10.3 Integrated Testing

1.2.3.10.3.1 Integrated Radionuclide Release: Tests and Models

June activities will be reported in a later monthly progress report.

1.2.3.10.3.2 Thermodynamic Data Determination

June activities will be reported in a later monthly progress report.

1.2.3.11 Integrated Geophysical Testing for Site Characterization

1.2.3.11.3 Geophysics - ESF Support, Subsurface Geophysical Testing

No significant activity. The work will resume when the capital and non-capital procurements have been received.

1.2.3.12 Waste Package Environment Testing

This WBS element was created from WBS element 1.2.2.2. Reporting and PACS have been converted to the new system, but funds still reside within WBS 1.2.2.

1.2.3.12.1 Chemical and Mineralogical Properties of the Waste Package Environment

The revised Study Plan 8.3.4.3.4.1 for Waste Package Geochemistry and Mineralogy that was sent to YMSCO is being reformatted to meet current format guidelines specified in the NRC-DOE Agreement. It will be submitted to YMSCO in July.

Work at the New Zealand natural process analog site is emphasizing evaluation of the way in which model validation activities can be conducted in the field. Data have been collected and compared against simulations which demonstrate that very good agreement can be achieved between the two. However, perfect matches are impossible due to inherent uncertainties in data values, thermodynamic property measurements, and limitations of conceptual models. As a result, attention is being focused on developing strategies that allow a more flexible approach to validation efforts. This will be important when validation efforts address characterization of processes and properties of the site.

Field-based experiments in New Zealand on dissolution and precipitation kinetics continue. Materials for sample holders have been emplaced in Paraiki Stream, in a pool at 89.1°C, pH 3.0, to evaluate the material durability. To date, all sample holder materials, except certain Fe- metals, have survived well. Mineral samples for kinetics measurements are ready for emplacement, once complete evaluation of sample holders is finished.

Collaborations continue with the University of Chicago and the University of Illinois, in areas of thermodynamic database review and development, and nuclear magnetic resonance (NMR) studies of cation exchange and sorption in minerals. A list of minerals for review has been developed and will be evaluated for consistency with other data bases.

1.2.3.12.2 Hydrologic Properties of the Waste Package Environment

Thermo-hydrological Calculations

In order to augment the thermo-hydrological calculation support of the thermal loading systems study, we have been conducting calculations in the near-field/altered zone hydrology task with the same set of thermal loading assumptions.

See WBS 1.2.1.5 for a description of the waste receipt scenario. In that section, we report on the impact of enhanced gas-phase diffusion on humidity and temperature and on the sensitivity of humidity at the end of boiling to matrix hydrological property data. In this section, we continue the sensitivity study to include temporal and spatial distributions of temperature and humidity.

Areal Mass Loadings (AMLs) of 24.2, 35.9, 55.3, 70, 83.4, 100, 110.5, and 150 MTU/acre were analyzed assuming the matrix hydrological properties given in the Reference Information Base (RIB) and Klavetter and Peters (1986), and in a recent draft report (Pruess and Tsang, 1994) which is based on measurements by Flint and others (1983).

Table 6 summarizes the time required to attain the indicated relative humidity, *RH*, at various repository locations and the temperature at which that value of *RH* is attained for the "reference" case based on the RIB and Klavetter and Peters data for AMLs of 55.3, 110.5, and 150.0 MTU/acre. It should be emphasized that the relative humidity calculations are based on the smeared-heat-source, disk-shaped model of the repository. Therefore, the relative humidity is based on average liquid saturation. It should also be noted that thermo-hydrological heterogeneity and variability in the heat output among the WPs will cause local behavior to deviate from average behavior.

Table 6								
Time required to attain the indicated relative humidity at various repository locations and the temperature at which that value of relative humidity is attained for 22.5-yr-old SNF, $k_b = 280$ millidarcy, and assuming the matrix properties from Klavetter and Peters (1986) for the TSw1 and TSw2 units.								
The locations are identified as the percentage of the repository area enclosed, with 0 percent corresponding to the repository center, and 100 percent corresponding to the outer perimeter								
Table 6a: AML = 55.3 MTU/acre								
Percentage of repository area enclosed (%)	Time required to attain the indicated relative humidity (yr)				Temperature at which the indicated relative humidity is attained (°C)			
	70%	80%	90%	95%	70%	80%	90%	95%
50	670	1660	3330	4630	107	97	80	72
75	410	940	1610	2280	107	99	89	81
90	NA	200	380	490	NA	103	97	94
97	NA	NA	NA	NA	NA	NA	NA	NA
Table 6b: AML = 110.5 MTU/acre								
Percentage of repository area enclosed (%)	Time required to attain the indicated relative humidity (yr)				Temperature at which the indicated relative humidity is attained (°C)			
	70%	80%	90%	95%	70%	80%	90%	95%
50	15,960	27,910	40,990	49,980	68	54	45	42
75	9540	15,520	24,950	32,590	76	64	53	48
90	3190	4890	7460	9890	93	82	73	68
97	1410	1810	2360	2890	106	101	93	88
Table 6c: AML = 150 MTU/acre								
Percentage of repository area enclosed (%)	Time required to attain the indicated relative humidity (yr)				Temperature at which the indicated relative humidity is attained (°C)			
	70%	80%	90%	95%	70%	80%	90%	95%
50	20,630	34,850	50,920	64,150	68	52	45	41
75	16,400	24,520	32,700	43,360	70	59	51	46
90	8660	12,090	16,520	19,780	81	72	64	59
97	4330	6020	8180	10,060	93	84	77	72

We repeated the repository-scale calculations for the five sets of matrix properties for the Topopah Spring welded tuff (Table 7) that are listed in Pruess and Tsang (1994) and based on Flint et al. (1993). For zero net recharge flux, the initial liquid saturation at the repository horizon is calculated to be 68, 76, 78, 74, 66, and 64% for the six cases in the table, respectively. In order to result in nearly the same initial liquid water content in the TSw1 and TSw2, a porosity (ϕ_m) of 0.11 was assumed for the three cases that yielded lower initial liquid saturation (reference case, LBL-USGS-3.4, and -3.3) and $\phi_m = 0.10$ for the three cases that yielded higher initial liquid saturations (LBL-USGS-3.5, -3.2, and -3.1/3.6).

Sample Name	S_r	ϕ_m	$k_{m,sat}$ (m^2)	α (10^{-9} Pa $^{-1}$)	m
Reference Case	0.08	0.11	1.9×10^{-18}	0.058	0.4438
LBL-USGS-3.2	0.0	0.10	4.0×10^{-16}	0.125	0.18
LBL-USGS-3.5	0.0	0.10	5.0×10^{-18}	0.133	0.25
LBL-USGS-3.1/3.6	0.0	0.10	1.0×10^{-18}	0.067	0.29
LBL-USGS-3.4	0.0	0.11	5.0×10^{-18}	0.067	0.25
LBL-USGS-3.3	0.0	0.11	4.0×10^{-18}	0.2	0.22

The properties listed are S_r , α , and m (the three van Genuchten characteristic curve fitting parameters), the matrix porosity (ϕ_m), and the saturated matrix permeability ($k_{m,sat}$).

For AMLs of 55.3, 110.5, and 150 MTU/acre, and for the five sets of LBL-USGS property measurements, Tables 8 through 10 summarize the relative humidity and temperature information given in Table 6 for the reference properties. Although these cases have different values of saturated matrix permeability, k_m , they all share the same bulk permeability, k_b , of 280 millidarcy. For an AML of 55.3 MTU/acre, relative to the case with the reference matrix properties (called the reference case), one of the LBL-USGS matrix property cases results in substantially faster re-wetting, one case results in nearly the same re-wetting rate, and three cases result in slower re-wetting back to ambient humidity conditions (98.4%) in the repository. A comparison of Tables 6a and 8a shows that LBL-USGS-3.2 results in substantially faster re-wetting back to humid conditions, resulting in relatively hot conditions as high relative humidity is attained. A comparison of Tables 6a and 8b shows that LBL-USGS-3.5 results in a similar re-wetting rate to the reference case. A comparison of Tables 8c-e with Table 6a shows that data from LBL-USGS-3.1/3.6 and -3.4 result in somewhat slower re-wetting, and that LBL-USGS-3.3 results in much slower re-wetting back to humid conditions. Regardless of the re-wetting rate, relatively hot conditions prevail for the 55.3-MTU/acre cases, (105 to 107°C) at the time that *RH* returns to 70%. In general, with the exception of LBL-USGS-3.2, there is not a great degree of variability in the relationship between temperature and *RH*.

Relative to the reference 110.5-MTU/acre case, one case results in substantially faster re-wetting, one case results nearly the same re-wetting rate, and three cases result in slower re-wetting back to ambient humidity conditions at the repository

Table 8: AML = 55.3 MTU/acre
 Time required to attain the indicated relative humidity at various repository locations and the temperature at which that value of relative humidity is attained for 22.5-yr-old SNF and $k_b = 280$ millidarcy. The locations are identified as the percentage of the repository area enclosed, with 0 percent corresponding to the repository center, and 100 percent corresponding to the outer perimeter.

Table 8a: Matrix properties for LBL-USGS sample 3.2 in the TSw1 and TSw2 units

Percentage of repository area enclosed (%)	Time required to attain the indicated relative humidity (yr)				Temperature at which the indicated relative humidity is attained (°C)			
	70%	80%	90%	95%	70%	80%	90%	95%
50	NA	750	1240	1480	NA	103	99	97
75	NA	280	700	870	NA	103	100	98
90	NA	NA	160	210	NA	NA	100	98
97	NA	NA	NA	NA	NA	NA	NA	NA

Table 8b: Matrix properties for LBL-USGS sample 3.5 in the TSw1 and TSw2 units

Percentage of repository area enclosed (%)	Time required to attain the indicated relative humidity (yr)				Temperature at which the indicated relative humidity is attained (°C)			
	70%	80%	90%	95%	70%	80%	90%	95%
50	490	1570	2520	3490	107	98	87	79
75	290	900	1350	1700	107	100	93	87
90	NA	190	330	400	NA	103	98	96
97	NA	NA	NA	NA	NA	NA	NA	NA

Table 8c: Matrix properties for LBL-USGS samples 3.1 and 3.6 in the TSw1 and TSw2 units

Percentage of repository area enclosed (%)	Time required to attain the indicated relative humidity (yr)				Temperature at which the indicated relative humidity is attained (°C)			
	70%	80%	90%	95%	70%	80%	90%	95%
50	690	2240	7170	12,050	107	90	65	57
75	430	1270	3340	5930	107	95	72	63
90	NA	220	450	640	NA	102	95	91
97	NA	NA	NA	NA	NA	NA	NA	NA

Table 8d: Matrix properties for LBL-USGS sample 3.4 in the TSw1 and TSw2 units

Percentage of repository area enclosed (%)	Time required to attain the indicated relative humidity (yr)				Temperature at which the indicated relative humidity is attained (°C)			
	70%	80%	90%	95%	70%	80%	90%	95%
50	870	2390	6660	10,600	106	89	67	59
75	510	1330	3210	5300	106	94	73	65
90	130	270	580	880	107	101	93	87
97	NA	NA	NA	NA	NA	NA	NA	NA

Table 8e: Matrix properties for LBL-USGS sample 3.3 in the TSw1 and TSw2 units

Percentage of repository area enclosed (%)	Time required to attain the indicated relative humidity (yr)				Temperature at which the indicated relative humidity is attained (°C)			
	70%	80%	90%	95%	70%	80%	90%	95%
50	960	3180	14,200	29,100	105	81	54	43
75	580	1790	7430	15,050	106	87	60	50
90	140	320	910	1910	107	99	86	72
97	NA	NA	NA	NA	NA	NA	NA	NA

horizon. A comparison of Tables 6b and 9a shows that LBL-USGS-3.2 results in much faster re-wetting back to ambient humidity conditions. Consequently, temperatures are significantly greater with respect to *RH*. For example, the center of the repository has a temperature of 96°C when *RH* returns to 70% as compared with 68°C in the reference case. A comparison of Tables 6b and 9b shows that LBL-USGS-3.5 results in nearly the same re-wetting rate as the reference case. Consequently, there is a similar relationship between temperature and *RH*. An

Table 9: AML = 110.5 MTU/acre

Time required to attain the indicated relative humidity at various repository locations and the temperature at which that value of relative humidity is attained for 22.5-yr-old SNF and $k_b = 280$ millidarcy. The locations are identified as the percentage of the repository area enclosed, with 0 percent corresponding to the repository center, and 100 percent corresponding to the outer perimeter.

Table 9a: Matrix properties for LBL-USGS sample 3.2 in the TSw1 and TSw2 units

Percentage of repository area enclosed (%)	Time required to attain the indicated relative humidity (yr)				Temperature at which the indicated relative humidity is attained (°C)			
	70%	80%	90%	95%	70%	80%	90%	95%
50	5970	6410	7060	8740	96	93	90	85
75	3480	3830	4170	4800	100	98	95	91
90	1760	2070	2440	2640	106	102	99	97
97	840	1120	1450	1720	107	103	100	98

Table 9b: Matrix properties for LBL-USGS sample 3.5 in the TSw1 and TSw2 units

Percentage of repository area enclosed (%)	Time required to attain the indicated relative humidity (yr)				Temperature at which the indicated relative humidity is attained (°C)			
	70%	80%	90%	95%	70%	80%	90%	95%
50	22,280	28,530	34,780	42,390	59	54	48	45
75	9580	12,710	17,200	23,350	75	68	61	55
90	2720	3680	4920	6760	97	89	82	75
97	1160	1530	1920	2290	107	103	98	93

Table 9c: Matrix properties for LBL-USGS samples 3.1 and 3.6 in the TSw1 and TSw2 units

Percentage of repository area enclosed (%)	Time required to attain the indicated relative humidity (yr)				Temperature at which the indicated relative humidity is attained (°C)			
	70%	80%	90%	95%	70%	80%	90%	95%
50	31,570	48,790	72,310	94,690	51	42	37	34
75	16,160	30,080	45,930	58,990	63	49	41	38
90	3450	6560	12,010	18,980	91	76	64	54
97	1130	1620	2260	2820	107	102	94	88

Table 9d: Matrix properties for LBL-USGS sample 3.4 in the TSw1 and TSw2 units

Percentage of repository area enclosed (%)	Time required to attain the indicated relative humidity (yr)				Temperature at which the indicated relative humidity is attained (°C)			
	70%	80%	90%	95%	70%	80%	90%	95%
50	31,290	47,260	71,840	93,860	51	43	37	34
75	16,470	29,220	44,140	57,350	62	50	42	38
90	3940	7260	12,780	19,080	87	74	62	54
97	1330	1830	2510	3490	107	100	91	83

Table 9e: Matrix properties for LBL-USGS sample 3.3 in the TSw1 and TSw2 units

Percentage of repository area enclosed (%)	Time required to attain the indicated relative humidity (yr)				Temperature at which the indicated relative humidity is attained (°C)			
	70%	80%	90%	95%	70%	80%	90%	95%
50	33,940	61,360	119,890	185,850	49	38	32	31
75	19,730	39,340	78,500	112,770	57	44	35	33
90	4770	11,340	26,180	39,140	83	65	49	42
97	1350	1990	3410	5360	107	98	84	74

examination of Tables 6b and 9c-d shows that LBL-USGS-3.1/3.6 and -3.4 result in very similar re-wetting rates that are substantially slower than the reference case in the inner 75% of the repository. For the outer 10% of the repository, these three cases have very similar re-wetting rates. Table 9e indicates that LBL-USGS-3.3 has a much slower re-wetting rate than all of the other cases, except at the outer 3% of the repository where re-wetting is modestly slower. For the inner 75% of the repository, LBL-USGS-3.1/3.6, -3.4, and -3.3 all have similar relationships between temperature and RH. For all six matrix property cases, the outer 3% of the

repository has a similar temperature versus *RH* relationship. Regardless of case, the outer 3% of the 110.5-MTU/acre repository is relatively hot (~106°C) at the time that *RH* returns to 70%. Except for LBL-USGS-3.2, the inner 75% of the repository has cooled to relatively cool temperatures (49 to 76°C at the time that *RH* returns to 70%.

Table 10: AML = 150 MTU/acre								
Time required to attain the indicated relative humidity at various repository locations and the temperature at which that value of relative humidity is attained for 22.5-yr-old SNF and $k_b = 280$ millidarcy. The locations are identified as the percentage of the repository area enclosed, with 0 percent corresponding to the repository center, and 100 percent corresponding to the outer perimeter.								
Table 10a: Matrix properties for LBL-USGS sample 3.2 in the TSw1 and TSw2 units								
Percentage of repository area enclosed (%)	Time required to attain the indicated relative humidity (yr)				Temperature at which the indicated relative humidity is attained (°C)			
	70%	80%	90%	95%	70%	80%	90%	95%
50	8960	9600	10,840	12,030	97	95	91	87
75	5690	6180	6830	8170	101	98	96	91
90	2980	3510	4060	4400	105	102	98	96
97	2020	2300	2650	2940	107	103	100	98
Table 10b: Matrix properties for LBL-USGS sample 3.5 in the TSw1 and TSw2 units								
Percentage of repository area enclosed (%)	Time required to attain the indicated relative humidity (yr)				Temperature at which the indicated relative humidity is attained (°C)			
	70%	80%	90%	95%	70%	80%	90%	95%
50	31,240	38,690	46,850	54,100	54	49	45	43
75	18,750	23,780	28,990	35,380	66	59	54	49
90	7740	9930	12,830	17,520	83	77	70	62
97	3480	4420	5820	8020	98	91	84	77
Table 10c: Matrix properties for LBL-USGS samples 3.1 and 3.6 in the TSw1 and TSw2 units								
Percentage of repository area enclosed (%)	Time required to attain the indicated relative humidity (yr)				Temperature at which the indicated relative humidity is attained (°C)			
	70%	80%	90%	95%	70%	80%	90%	95%
50	36,740	54,710	76,450	103,600	50	42	38	35
75	29,790	46,930	67,180	81,860	52	43	38	36
90	13,140	23,350	36,290	47,780	70	55	45	41
97	4630	7810	13,500	21,390	90	77	65	55
Table 10d: Matrix properties for LBL-USGS sample 3.4 in the TSw1 and TSw2 units								
Percentage of repository area enclosed (%)	Time required to attain the indicated relative humidity (yr)				Temperature at which the indicated relative humidity is attained (°C)			
	70%	80%	90%	95%	70%	80%	90%	95%
50	36,240	53,670	77,150	106,290	51	43	38	35
75	28,920	44,800	65,090	79,720	53	44	39	36
90	13,070	22,110	34,020	44,680	70	57	47	42
97	4970	7960	12,920	19,230	88	77	66	57
Table 10e: Matrix properties for LBL-USGS sample 3.3 in the TSw1 and TSw2 units								
Percentage of repository area enclosed (%)	Time required to attain the indicated relative humidity (yr)				Temperature at which the indicated relative humidity is attained (°C)			
	70%	80%	90%	95%	70%	80%	90%	95%
50	38,530	67,740	136,540	224,430	49	40	34	32
75	31,910	56,830	111,490	171,140	51	40	34	33
90	16,730	32,050	60,180	86,980	63	48	38	35
97	6120	11,790	23,940	36,410	83	68	52	44

Relative to the reference property 150-MTU/acre case, one of the LBL-USGS matrix property cases results in substantially faster re-wetting, one case results in nearly

the same re-wetting rate, and three cases result in slower re-wetting back to ambient humidity conditions at the repository horizon. A comparison of Tables 6c and 10a shows that LBL-USGS-3.2 results in much faster re-wetting back to ambient humidity conditions. Consequently, temperatures are significantly greater with respect to *RH*. For example, the center of the repository has a temperature of 97°C when *RH* returns to 70% as compared with 68°C in the reference case. A comparison of Tables 6c and 10b shows that LBL-USGS-3.5 results in nearly the same re-wetting rate as the reference case. Consequently, there is a similar relationship between temperature and *RH*. An examination of Tables 6c and 10c-d shows that LBL-USGS-3.1/3.6 and -3.4 result in very similar re-wetting rates that are substantially slower than the reference case in the inner 75% of the repository. For the outer 10% of the repository, these three cases have similar re-wetting rates. Table 10e indicates that LBL-USGS-3.3 has a much slower re-wetting rate than all of the other cases throughout the entire repository. Re-wetting back to *RH* = 90 and 95% is particular slow for these property data. Unlike the 55.3- and 110.5-MTU/acre cases, the slower re-wetting rates for LBL-USGS-3.1/3.6, -3.4, and -3.3 for the 150 MTU/acre AML allow the outer 3% to cool to somewhat cooler temperatures (83 to 90°C) when *RH* returns to 70%. With the exception of LBL-USGS-3.2, the inner 75% of the repository has cooled to relatively cool temperatures (51 to 70°C) at the time that *RH* returns to 70%, and to 40-59°C at the time that *RH* returns to 80%.

Two critical questions for waste package (WP) integrity are:

- For humid conditions, what temperature is sufficiently cool to result in a substantial reduction in WP degradation rates?
- For hot conditions, what relative humidity is sufficiently dry to result in a substantial reduction in WP degradation rates?

The answer to these questions will be addressed by the WP material characterization studies that will determine the range of temperature and relative humidity conditions that are sufficiently cool and/or dry to result in significantly reduced degradation rates for the WP materials under consideration.

Some of the properties listed in Table 7 have stronger influence on the results than other listed properties. In general, liquid phase re-wetting increases with increasing $k_{m,sat}$ and m , and with decreasing α . Gas phase re-wetting is primarily affected by τ_{eff} (see Section 1.2.1.5). Tables 6, 8, 9 and 10 show that the re-wetting was almost identical for the LBL-USGS-3.1/3.6 and -3.4 property sets, and it should be noted that a five fold increase in saturated matrix permeability was offset by a small decrease in the fitting factor, m , from 0.29 to 0.25.

The calculations reported here assume a binary gas-phase diffusion tortuosity factor, τ_{eff} , of 0.2. Next month, we will report on repeating much of the above suite of cases for the situation of enhanced gas-phase diffusion where it is assumed that $\tau_{eff} = 2$. Section 1.2.1.5 of this month's report discusses recent results in an ongoing study of the impact of gas-phase diffusion using the reference matrix properties.

Laboratory Experiments

Electrical Impedance as a Function of Moisture Content

During June, we continued the preparation of more samples from the G-4 hole and the Large Block Test cores to complete the measurements at 95°C. Analysis of the existing data indicates that the frequency dependent measurements may be useful in describing the manner in which water wets rock. Several conduction mechanisms are observed that change in importance with changing saturation levels. These mechanisms are being studied.

Characteristic Curves of Tuff

For the experiment of determining the moisture retention curve and one-dimensional imbibition using G-4 core, we continued the moisture retention experiments at high temperatures. Measurements at 95°C and about 95% relative humidity were completed. The samples are being saturated to 100%, and the measurements in the drying phase will start soon.

The Effect of Confining Pressure on Fracture Healing

We continued the experiment to determine the effect of confining pressure on fracture healing, as observed previously by Lin and Daily. A fractured Tcpopah Spring tuff sample from the G-4 hole is used. Permeability as a function of temperature, at a confining pressure of 1 MPa and pore pressure of 0.5 MPa, is being determined. We have completed the measurements up to 150°C and back down to 25°C. After heating, the water permeability at 25°C is about 50% lower than that measured at the same temperature before heating. No drastic fracture healing has been observed. Steam flow was performed at 125°C; and no significant effect on the permeability was observed. All the chemical data measured on water samples after flow through the rock have been entered into a database. Some water samples were examined for the existence of bacteria, and no evidence of bacteria colonies was observed.

Water permeability was measured at an effective pressure of 1.5 MPa (2.0 MPa confining pressure and 0.5 MPa pore pressure) with 25, 50, and 80°C temperatures. The measurements will be continued up to 150°C.

1.2.3.12.3 Mechanical Attributes of the Waste Package Environment

Management and Integration

S. Blair attended the IHLRWM conference in Las Vegas (May 24-26) and the 1st North American Rock Mechanics Symposium in Austin, TX (June 3-5). P. Berge attended the Spring AGU meeting (May 23 - 27). The purpose of attending these meetings was to participate in geomechanics sessions on deformation and fluid flow behavior of rock at repository conditions.

Budget plans for the remainder of year were developed.

Planning documents

Activity Plan AP-GM-01/GM-03/GM-05 for the Geomechanical Attributes of the Waste Package Environment was completed and issued as a controlled document.

S. Blair assisted the P.I. in review and resolving geomechanics-related comments on Study Plan 8.3.4.2.4.4 (Engineered Barrier System Field Tests).

Laboratory

The Waste Package Design Integration Team toured the laboratory facilities.

Preparation of test specimens from core samples taken from the Large Block Test was initiated. Equipment such as thermocouples, electrical conditioning boxes, etc. for laboratory tests on small blocks was ordered.

Support of the Large Block Test (LBT)

Development of a Multipoint Borehole Laser EXtensometer (MBLEX) design continued, and several component parts for this system were ordered. This system was discussed with representatives of AECL, USBM, Bechtel Corp., and other interested parties to evaluate potential collaborations in its development.

Preliminary arrangements were made with SAIC regarding use of their seismic source for elastic wave velocity measurements on the LBT.

Modeling

The FRACROCK code was used to assess the stability of the rock bolting system to be used at the LBT. Analysis shows the stresses in the rock to be quite low, indicating that the bolting system should be stable.

A preliminary map of fractures in the horizontal plane of the block was digitized for input into the DDA discrete analysis code. Digitizing the fracture map that represents the top surface of the block was initiated.

1.2.3.12.4 Engineered Barrier System (EBS) Field Tests

Revisions to the Engineered Barrier System Field Tests (EBSFT) Study Plan are in progress based on the comment resolution meeting.

Large Block Test (LBT)

Matrix Bulk Porosity

A total of 19 Hg-porosimetry measurements have been completed using the core sections from the vertical instrument holes. The average bulk porosity is about 11.24%, with a minimum value of 8.23% and a maximum value of 16.17%.

Fracture Mapping

The fractures at the top of the block were mapped and described in detail. We are evaluating Earth Vision as a tool to display the data in 3-D.

Excavation

The excavation work continued. The area 1 m away from the block was excavated to about 3 m below the top of the block. Some small samples were collected for testing of moisture content.

Small Block Tests in the Laboratory

Tests continued on the performance of the Kapton heaters (to be used as guard heaters for the large block and as heaters for the small block experiments), the potential insulation materials, and the thermal control for the guard heaters, under a 5 MPa stress. Copper plates may be used to distribute heat from the guard heaters. Tests continued to evaluate the lateral temperature distribution on the surface of a copper plate, opposite to the heater. Thermal conduction model calculations continued to help design the guard heaters.

Preparation of small blocks, obtained from Fran Ridge, for scoping experiments continued. X-ray imaging to determine water saturation began.

The Load Retaining Frame

Engineering analysis of the capability of the load retaining frame, as designed, was completed. The load retaining frame design is not structurally adequate to contain the desired pressure of 600 psi. The predicted stress levels in gussets of the frame exceed the yield and ultimate strengths of the frame material. The axial loads in the bolts have small margins as compared to the yield and ultimate strengths of the bolt material. Finally, there is a significant vertical displacement between the bottom and top of the frame. Modifications were proposed to retrofit the frame. Those modifications include:

- decreasing the distance from the cylinder walls to the bolts by drilling new holes in the flanges nearer the walls and increase number of bolts for those new holes,
- adding a c-shape collar assembly to the hoop direction vertical flanges,
- stiffening the gussets,
- adding a stiffening collar around the bottom flange to reduce loads on the anchor bolts, and
- to connect the load retaining frame to the bladder support structures inside the frame.

The effectiveness and associated cost of these modifications are being evaluated.

Aircraft Engineering Corporation, the fabricator of the frame, reported that they are having difficulty in completing the frame construction within the price and time allocated under the contract. Negotiation with Aircraft Engineering is underway to resolve the problem.

Loading Devices

A meeting with the potential manufacturer for the bladders was held to discuss detailed design criteria of the bladders. The engineering design of the bladder support/housing devices continued.

Other Items

Procurement of instruments continued.

SNL continued mapping the fracture flow visualization test area along with the excavation.

A poster paper entitled "A Medium Scale Test of the Thermal Effect on Hydrological-Chemical-Mechanical Processes in a Rock Mass", by W. Lin, et al., was presented at the First North American Rock Mechanics Symposium.

1.2.3.12.5 Characterization of the Effects of Man-Made Materials on Chemical & Mineralogical Changes in the Post-Emplacement Environment

June activities will be reported in a later monthly progress report.

1.2.5 REGULATORY

1.2.5.1 Regulatory Coordination and Planning

J. Johnson attended the YMP-Radionuclide Solubility Working Group (SOLWOG) meeting in Las Vegas on June 2. He described the means by which SOLWOG members could access GEMBOCHS databases and software tools via remote access. LLNL staff are currently in the process of establishing these remote-access links.

1.2.5.2 Licensing

1.2.5.2.2 Site Characterization Program

R. Van Konynenburg attended a "dry run" on June 28 in Las Vegas in preparation for a talk he is scheduled to deliver to the NWTRB in July. The subject is "Potential Effects of Engineered Barriers on Radionuclide Migration". His talk will focus on identification and discussion of the corrosion products that would be produced on the various metal barrier materials (and other components in the waste package, such as the pour canister, multi-purpose container for spent fuel and the basket material) and how these corrosion products will interact with the various radionuclides that will be present. Certain metals and corrosion products will sorb some radionuclides, and the beneficial interaction will be discussed in addressing controlled release issues. R. Van Konynenburg also assisted LANL personnel in preparing their talk on the release of Carbon-14.

1.2.5.3 Technical Data Management

1.2.5.3.4 Geologic and Engineering Materials Bibliography of Chemical Species (GEMBOCHS)

The first edition of the new, stand-alone GEMBOCHS Data Catalog for the YMP-TDB was generated. This quarterly catalog, which covers the second quarter of 1994, includes an overview of the GEMBOCHS system, a discussion of recent accomplishments, and tables summarizing

- The types of thermodynamic data contained in GEMBOCHS,
- the specific chemical species and data contained in each of the seven thermodynamic data files currently provided for use with EQ3/6, and
- the literature sources for these data.

The R24 suite of thermodynamic data files for use with EQ3/6 has been completed. This suite incorporates improved thermodynamic data for several key aluminum aqueous species and aluminosilicates.

A revised set of element catalogs has been generated. The catalogs contain all thermodynamic data available in GEMBOCHS for compounds of the elements Tc, Th, U, Np, Pu, and Am. The catalogs are now available for remote electronic access via the anonymous GEMBOCHS ftp account.

Jewel code development: Several minor computational bugs associated with generation of thermodynamic data files for use with the geochemical modeling code *React* were resolved.

1.2.5.3.5 Technical Data Base Input

No significant activities.

1.2.5.4 Performance Assessment

1.2.5.4.2 Waste Package Performance Assessment

June activities will be reported in a later monthly progress report.

1.2.5.5. Special Projects

1.2.5.5.1 Integrated Test Evaluation (ITE)

This activity has not been funded in FY94.

1.2.5.5.2 Energy Policy Act Support

No significant activity.

1.2.9 PROJECT MANAGEMENT

1.2.9.1 Management and Coordination

1.2.9.1.2 Technical Project Office Management

W. Clarke, C.K. Chou, and J. Savy met with L. Hayes, J. Whitney (USGS) and staff on July 6 in Denver. The purpose of the meeting was to discuss the future involvement of LLNL in YMP seismic hazard assessment work.

A. Simmons (YMSCO), visited LLNL-YMP on July 7 to work on program planning.

W. Clarke and J. Blink attended the TAG meeting in Las Vegas on June 24.

J. Blink participated in the 50% design review of the Integrated Data and Control System on June 7.

J. Blink taught the physics module for the Nye County LESSON (science workshop for teachers) at NTS on June 1. He also taught the electromagnetism module and assisted A. Gil (YMSCO) in teaching the earth science modules on June 2-3. On June 8, he and J. Calovini (RSN) served as tour guides for both the Weapon and Yucca Mountain sides of NTS for the Nye County teachers. On June 13-14, J. Blink taught the physics module for the Clark County LESSON workshop. He served as tour guide on June 17. He also taught the electromagnetism module and worked with E. Harle (SAIC) to teach the earth science module on June 22-23.

On June 15, J. Blink presented hands-on science classes to 40 eighth grade students attending the Math, Science, & Engineering Academy for predominantly black school. The summer course is co-sponsored by DOE-NV and by Ft Valley State College in Georgia.

1.2.9.2 Project Control

1.2.9.2.2 Participant Project Control

Actual schedule progress and costs were submitted to the PACS reporting system via the PACS workstation. Variance analysis explanations were developed.

1.2.11 QUALITY ASSURANCE

Quality Assurance Coordination and Planning

The LLNL-YMP Quality Procedures (QPs) are being reviewed and edited to incorporate text and procedural changes required by the YMSCO review of the QARD requirements matrix. Royce Monks traveled to Las Vegas during the week of June 6 to discuss changes made thus far with YMSCO personnel.

Quality Assurance Program Development

The YMP Quality Procedures are being revised to comply with QARD review. Changes are made to the RTN matrix during the process to maintain consistency.

Quality Assurance Verification

Quality Assurance Verification - Audits

Notification of Audit 94-06 was distributed on June 17, and an entrance meeting was conducted on June 29. This audit will concentrate on LLNL-YMP Performance Analysis and include the following procedures/requirements:

- 033-YMP-QP 2.4, Technical Reviews
- 033-YMP-QP 2.6, Readiness Reviews
- 033-YMP-QP 2.8, Quality Assurance Grading
- 033-YMP-QP 2.10, Qualification of Personnel
- 033-YMP-QP 3.0, Scientific Investigation Control
- 033-YMP-QP 3.2, Software Quality Assurance
- 033-YMP-QP 3.4, Scientific Notebooks
- 033-YMP-QP 5.0, Technical Implementing Procedures
- 033-YMP-QP 8.0, Identification & Control of Items, Samples & Data
- 033-YMP-QP 9.0, Control of Processes
- 033-YMP-QP 13.0, Handling, Storage and Shipping

Corrective action for CAR LLNL-032 was completed and verified, and the CAR was closed on June 13.

Quality Assurance Verification - Surveillance

No significant activity.

Field Quality Assurance/Quality Control

No significant activity.

Quality Assurance - Quality Engineering

No significant activity.

1.2.12 INFORMATION MANAGEMENT

1.2.12.2 Records Management

1.2.12.2.2 Local Records Center Operations (LRC)

LLNL-YMP Document Control issued seven revisions and one change notice. Follow up continues on previously distributed documents.

1.2.12.2.3 Participant Records Management

A total of 147 items were logged into the LLNL-YMP tracking system. This includes twenty-five records/records packages that were processed through to the CRF. Six action items were closed.

1.2.12.2.5 Document Control

LLNL received no funding under this WBS element for FY94. Work performed to complete LLNL's obligation in this WBS element is funded under WBS 1.2.12.2.2.

1.2.13.2 SAFETY AND OCCUPATIONAL HEALTH

1.2.13.2.5 Occupational Safety and Health

J. Blink performed two ES&H inspections at the Fran Ridge site of the Large Block Test. Documentation was delivered to the Safety Office in the FOC.

1.2.15 SUPPORT SERVICES

1.2.15.2 Administrative Support

No significant activity.

1.2.15.3 Yucca Mountain Site Characterization Project (YMP) Support for the Training Mission

Currently there are 102 participants on the project who are to be trained and/or tracked. Three new staff members and three summer hires were oriented in June.

Creation of a new training database program is in progress. Programming has been completed; however, the database needs to be tested and implemented. The projected completion date is now August.

LLNL PROJECT STATUS REPORT EXTERNAL DISTRIBUTION

June 1994

PRELIMINARY STAMP

Dr. J. Bates Chemical Technology
Argonne National Laboratory
9700 S. Cass Avenue
Argonne, Illinois 60439

H. Benton
M&O, M/S 423
101 Convention Center Drive
Las Vegas, NV 89109

A. Berusch (RW-20)
OCRWM
Forrestal Building
Washington, DC 20585

M. Bishop
YMSCO
US Department of Energy
101 Convention Center Drive
Las Vegas, NV

M. Blanchard
YMSCO
US. Department of Energy
P.O. Box 98518
Las Vegas, Nevad 89193-8518

J. Blink
LLNL/Las Vegas
101 Convention Center Drive, Suite 880
Las Vegas, NV 89109

S. Bodnar
TRW, M/S 423
101 Convention Center Drive
Las Vegas, Nevada 89109-2005

B. Bodvarsson
LBL/Earth Sciences
Bldg. 50 E
1 Cyclotron Road
Berkeley, CA 94720

M. Brodeur
Science Applications Int'l Corp.
101 Convention Center Dr., #407
Las Vegas, NV 89109-2005

S. Brocoum
YMSCO
101 Convention Center Dr.
Las Vegas, NV 89109

J. Canepa
Los Alamos National Laboratory
P.O. Box 1663/N-5, MS J521
Los Alamos, NM 87545

P. Cloke
Science Applications Int'l Corp.
101 Convention Center Dr., #407
Las Vegas, NV 89109-2005

C. Conner
DOE, RW-133
1000 Independence Ave., SW
Washington, DC 20585

G. Cook
YMSCO
U.S. Department of Energy
P.O. Box 98518
Las Vegas, NV 89193-8518

W. Dixon
YMSCO
U.S. Department of Energy
P.O. Box 98518
Las Vegas, NV 89193-8518

T. Doering
M&O
101 Convention Center Dr., MS 423
Las Vegas, NV 89109

J. Dyer
YMSCO
U.S. Department of Energy
P.O. Box 98518
Las Vegas, NV 89193-8518

PRELIMINARY STAMP
R. Einziger
Battelle-Pacific Northwest
P.O. Box 999/MS P714
Richland, WA 99352

R. Fish
M&O
101 Convention Center Dr., M/S 423
Las Vegas, NV 89109

L. Foust
Technical Project Officer
CRWMS M&O, M/S 423
101 Convention Center Dr.
Las Vegas, NV 89109

R. Green
Southwest Research Institute
6220 Culebra Rd.
San Antonio, TX 78238-5166

L. Hayes
U.S. Geological Survey
Box 25046/MS 425
Denver Federal Center
Denver, CO 80225

R. Hughey
Nuclear Energy Division
US DOE/OAK
1301 Clay St., Rm. 700-N
Oakland, CA 94612

S. Kennedy
OCRWM
Forrestal Bldg.
Wash., D.C. 20585

V. Iorri
YMSCO
U.S. Department of Energy
P.O. Box 98518
Las Vegas, Nevada 89193-8518

C. Johnson
M&O
101 Convention Center Dr. M/S 423
Las Vegas, NV 89109

S. Jones
YMSCO
U.S. Department of Energy
101 Convention Center Dr.
Las Vegas, NV 89109

N. White (3)
Nuclear Regulatory Commission
301 E. Stewart Ave. #203
Las Vegas, NV 89101

H. Kalia
Los Alamos National Laboratory
101 Convention Center Dr., Suite 820
Las Vegas, NV 89109

PRELIMINARY STAMP
S. Marschman, P7-14
Battelle, Pacific Northwest
P.O. Box 999
Richland, WA 99352

M. Martin
TRW, M/S 423
101 Convention Center Dr.
Las Vegas, NV 89109-2005

S. Nelson
M&O
101 Convention Center Dr., M/S 423
Las Vegas, NV 89109

J. Dyer
YMSCO
U.S. Department of Energy
P.O. Box 98518
Las Vegas, NV 89193-8518

PRELIMINARY STAMP
R. Einziger
Battelle-Pacific Northwest
P.O. Box 999/MS P714
Richland, WA 99352

R. Fish
M&O
101 Convention Center Dr., M/S 423
Las Vegas, NV 89109

L. Foust
Technical Project Officer
CRWMS M&O, M/S 423
101 Convention Center Dr.
Las Vegas, NV 89109

R. Green
Southwest Research Institute
6220 Culebra Rd.
San Antonio, TX 78238-5166

L. Hayes
U.S. Geological Survey
Box 25046/MS 425
Denver Federal Center
Denver, CO 80225

R. Hughey
Nuclear Energy Division
US DOE/OAK
1301 Clay St., Rm. 700-N
Oakland, CA 94612

S. Kennedy
OCRWM
Forrestal Bldg.
Wash., D.C. 20585

V. Iorii
YMSCO
U.S. Department of Energy
P.O. Box 98518
Las Vegas, Nevada 89193-8518

C. Johnson
M&O
101 Convention Center Dr. M/S 423
Las Vegas, NV 89109

S. Jones
YMSCO
U.S. Department of Energy
101 Convention Center Dr.
Las Vegas, NV 89109

N. White (3)
Nuclear Regulatory Commission
301 E. Stewart Ave. #203
Las Vegas, NV 89101

H. Kalia
Los Alamos National Laboratory
101 Convention Center Dr., Suite 820
Las Vegas, NV 89109

PRELIMINARY STAMP
S. Marschman, P7-14
Battelle, Pacific Northwest
P.O. Box 999
Richland, WA 99352

M. Martin
TRW, M/S 423
101 Convention Center Dr.
Las Vegas, NV 89109-2005

S. Nelson
M&O
101 Convention Center Dr., M/S 423
Las Vegas, NV 89109

J. Younker
M&O/TRW
101 Convention Center Dr.
Las Vegas, NV 89109

P. Zielinski
YMSCO
U.S. Department of Energy
P.O. Box 98518
Las Vegas, Nevada 89193-8518